Tesi di Dottorato di Ricerca

in Automatica, Bioingegneria e Ricerca Operativa

Ciclo XXX

Analysis and modeling of the EEG activity and connectivity in post-stroke conditions

Dipartimento di Ingegneria Informatica, Automatica e Gestionale 'Antonio Ruberti'

Candidato

Dott. Stefano Caschera

Relatore

Prof.ssa Laura Astolfi

Esame finale anno 2018

Table of Contents

Introduction

Understanding the mechanisms of brain development and training is an important topic in neuroscience research. One of the most remarkable abilities of the brain is to adapt to the events of life. The brain is a dynamic organ that evolves throughout life. During learning and experiencing, it is the structure of the brain itself that changes, with the creation of new connections between neurons. Neuroplasticity is not an isolated state of the nervous system, it is a normally continuous state. That is because the brain is meant to respond to changes in environmental conditions or because of pathological conditions of different aetiology. Exercising and practice have long been used to restore (to varying degrees) impaired functions. Improved training strategies, rehabilitative protocols and methodologies to foster the neuroplasticity effects are currently being developed. The improvement in our understanding of the neuroplastic changes associated with injuries and the inherent repair strategies is of crucial importance. A key question is to evaluate whether and to what extent a certain rehabilitation strategy is actually helping the neuroplasticity process.

In the clinical practice, in addition to their importance for the diagnosis of motor and cognitive impairment, behavioural scales are used as well to assess the impact of the brain reorganization induced by neurorehabilitative interventions. Although there are numerous general and specific scales with established reliability and validity, no single scale is suitable to all clinical or research situations. Furthermore, behavioural scales provide an indirect measure of brain plasticity through its behavioural manifestations, but not directly in the brain. Indeed, finding markers that could predict and enhance brain plasticity is still a challenge. However, research on biomarkers of recovery is still limited, especially using neurophysiological tools.

Despite the enormous potential given by recent advances in sensor and signal processing technology, the information provided by these investigations has not yet been effectively used in the clinical field due to the difficulty in extracting stable and synthetic indices. Developments aimed at overcoming this limitation could lead to the definition of descriptors that can be related to clinical parameters of interest for the diagnosis, the understanding and the evaluation of the effects of neuro-rehabilitation therapies.

The overall objective of my PhD project has been to establish a methodology for the definition and analysis of neurophysiological indices that can provide a measure of changes in brain activity and organization that can be quantifiable (i.e. measurable in real world conditions), is reliable (sensitive, specific, and consistent over time), widely applicable and modifiable (amenable to improvement using existing approaches). The aim is to describe the specific properties of the general brain organization to be correlated with the outcome of the rehabilitation intervention, with possible prognostic/decision support value. The objective is to support the diagnosis of motor and cognitive disabilities, to provide a neurophysiological description of the changes in brain activity and organization that underlie functional recover and to allow the evaluation of the effects of rehabilitative treatments (conventional and innovative) in terms of brain reorganization (measures of neurophysiological outcome of a treatment).

To this purpose, my research activity has focused on developing an approach for the extraction of neurophysiological indices from a non-invasive estimate of brain activity and connectivity based on electroencephalographic (EEG) measurements.

High Density EEG offers advantages such as high safety and affordability in medical settings, especially in those that are traditionally difficult, such as stroke. Brain injuries represent major medical unmet needs

worldwide and need the development of new therapies. Given the insidious nature of these conditions and the significant cost of many diagnostic tests, there is a strong need for a method that is widely available, reliable and inexpensive. In this regard, the EEG can have significant potential and many considerable advantages. The EEG has an excellent temporal resolution, of the order of a few milliseconds, thus reflects synaptic activity, which is a common denominator for the functional impact of neurodegenerative processes. EEG is a non-invasive, portable and inexpensive technology that is widely adopted and that requires a relatively short acquisition time. Computerized Tomography (CT) and Magnetic Resonance Imaging (MRI) currently make it possible to easily obtain accurate measurements of neural lesions. This is not, however, the case for measuring brain function. Although functional MRI, Positron Emission Tomography (PET) and other associated methods can be used to assess brain function, these neuroimaging techniques have major limitations for large-scale clinical adoption, including cost, accessibility and safety. Moreover, although it has a much lower spatial resolution than the other methods mentioned above, electroencephalography is one of the few techniques to study neuronal activity in a non-invasive manner with a timing that corresponds to that of the processes under study.

Major attention has been given to the analysis of EEG recorded during the resting state. EEG measures of resting brain function provide insights into basal differences in brain state, therefore useful to predict the capacity of an individual brain, transcending inter-individual heterogeneity, to undergo plasticity and thus respond to therapeutic intervention.

All data reported in this thesis were collected by the team of the Neuroelectrical Imaging and BCI Lab (NEILab) at Fondazione Santa Lucia, IRCCS, Rome, Italy.

This thesis is divided into five Chapters. Chapter 1 describes the general physiological aspects of the nervous system, the neuronal electrophysiology,

the electroencephalography techniques and the monitored activity of the brain in order to understand the brain dynamics when the subject is engaged in particular experimental tasks. In Chapter 2, methods for the estimation of cortical connectivity based on auto-regressive multivariate models are presented, as well as methods for validation of connectivity estimates. These connections are then used to generate network data for further analysis such as graph theory metrics. Graph theory provides tractable means to analyze dynamic and integrated systems. In Chapter 3, the topographic reorganization after a stroke event of the brain connectivity network related to the resting state condition was described by defining various indexes. Differences in brain network organization have been investigated with respect to a healthy population and between different subgroups of patients in order to evaluate the deviation from the healthy condition and characterize patients on the basis of their clinical features. Chapter 4 describes a study conducted on the EEG tracks of a group of stroke patients undergoing motor imaging training supported by a Brain Computer Interface (BCI). Through spectral and connectivity estimation analysis, the study aimed to prove and characterize the amount of recovery of patients undergoing rehabilitation training based on motor imagery. In Chapter 5, it was explored whether an EEG-derived connectivity sensorimotor index at rest could vary in relation with the corticospinal tract integrity and excitability in subacute stroke patients. Functional changes in the motor area have been quantified and positively correlated with commonly used stroke clinical indices. As for today, the uncertainties about the effects of in-homogeneities due to brain lesions preclude the adoption of EEG functional mapping on patients with lesioned brain. In Chapter 6, is described a work that has the aim to quantify the accuracy of a distributed source localization method in recovering extended sources of activated cortex when cortical lesions of different dimensions are introduced in simulated data. To this purpose, EEG source-

distributed activity estimated from real resting state data was modified including silent lesion areas. Finally, a general conclusion, reporting the main contributions achieved within this PhD project, their possible impact and their future development, closes this PhD thesis.

I

Physiological bases and characteristics of the Electroencephalographic signal

---

_____

1.1 The central nervous system

The human brain is the central organ of the human nervous system, it is the primary location of most of the psychic and neurological functions of the body. Its complexity can be quantified by comparing it to a network interconnecting 10^{10} neuronal cells. Each of them is capable of very simple operations: depending on the state of polarization of the neurons connected to it, the neuron may (or may not) depolarize, thus providing an electrochemical signal to the connected neurons. These will become responsible for the transmission and processing of the information through the nervous system.

The distinction between the central and peripheral nervous systems is for merely didactic purposes, since the peripheral nervous system (PNS) consists mainly of extensions of nerve cells that are part of the central nervous system (CNS). Therefore, the following definition applies by convention: the CNS represents all nerve formations contained within the cranial cavity and the vertebral canal.

The central nervous system is a bilateral and symmetrical structure, traditionally divided into six parts: spinal cord, medulla, pons and cerebellum, midbrain, diencephalon and cerebral hemispheres. All brain functions are located in the cortex, which covers the cerebral hemispheres and in which all information is processed and integrated. The cortex, in itself, is a very complex structure whose morphology, intensely irregular, is the result of the particular brain evolution of the primates. In fact, during this evolution, the volume of the cortex has increased more rapidly than the volume of the skull, forming a large number of slits (called sulci) and circumvolutions, whose crests are called gyri. Some of the sulci are always present in the human brain, so they are used as reference points to divide the cortex of each hemisphere into four lobes: frontal, parietal, temporal and occipital (Figure 1.1).

Among the structures that compose the nervous system, the cerebral cortex is certainly the part that has developed most recently and certainly characterized by a high degree of complexity.
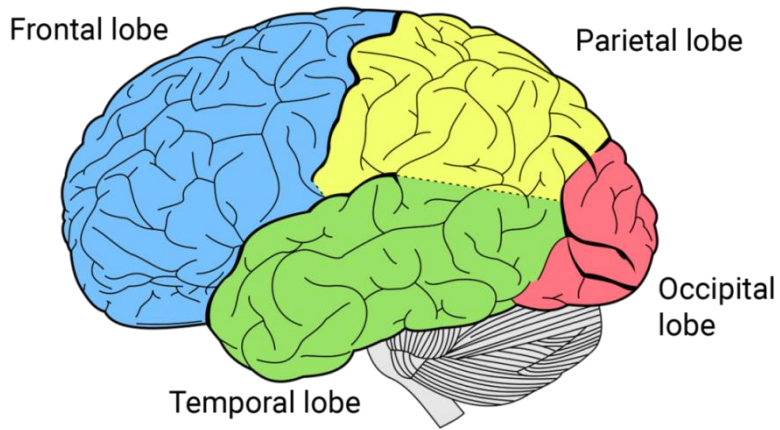
Fig. 1.1 - Schematic representation of brain structure.

It has long been known that different areas of the brain are related to specific cognitive and motor tasks: in literature a widely used subdivision of the cerebral cortex is that of German anatomist Korbinian Brodmann that, by performing accurate histological examinations and evaluating different types of nerve cells and myelin fibre placement, identified 47 specific areas with distinct characteristics. In Figure 1.2 it is possible to distinguish various areas that refer to some specific tasks, such as the primary sensory area (3-1-2), the secondary sensory area (5-7), the primary visual area (17), the secondary visual area (18-19), the primary motor area (4) and the premotor area (6).
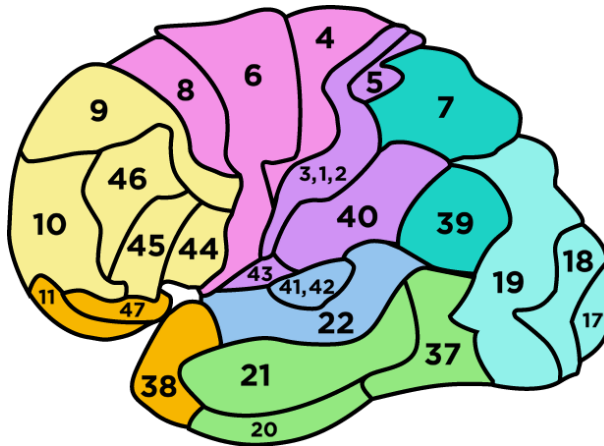
Fig. 1.2 - Brodmann areas on the representation of the brain. Each numbered zone is associated with a portion of the brain in which the neurons are similar.

1.2 The cortical neurons

Electroencephalography (EEG) measures voltage fluctuations mainly generated by the grey matter of the cortex but it is also influenced by the grey matter placed deeper (e.g. thalamus). The cerebral cortex contains different types of nerve cells (neurons), whose structure is represented in Figure 1.3, responsible for the processing and transmission of information in the nervous system.
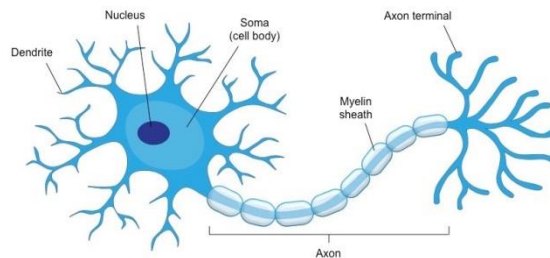
Fig. 1.3 The cell structure that contains the nucleus controls the metabolism of the whole unit; the dendritis receives the incoming impulses while the propagation of the nerve impulses takes place through the axon that is covered by the myelin sheath. The electrical signal is transmitted through the inter-neuronal synapses.

Depending on their morphology, their laminar arrangement and the class of neurotransmitters they use, nerve cells can be grouped into two main categories. A particular type of cell, the pyramidal cell, is the first class to be considered. These cells represent, with their pyramid-shaped cell bodies, but especially with their multiple connections, the main constituent of the cerebral cortex. Pyramidal cells project their axons to other brain regions and to the spinal cord; they are excitatory neurons and constitute the main projection neurons of the cerebral cortex. These have collateral ramifications that have a significant functional role in the generation of global electrical activity of the neural cortical aggregates. These cells have a characteristic dendritic organization that facilitates the integration of various adjoining signals. In fact, their apical dendrites often cross several cortical layers and are always oriented perpendicularly to the cortical surface. This anatomical organization means that afferent synaptic connections from different cortical layers reach the dendritic tree at different points. The other class of cells within the cerebral cortex is generically defined as non-pyramidal cells. Non-pyramidal cells have oval shaped cell bodies. In general, their axons do not leave the cortex but terminate on nearby neurons; for this reason they are called interneurons. From a morphological point of view, interneurons constitute a heterogeneous population. By far, the largest group consists of stellate cells. A stellate cell has the axon oriented vertically, parallel to the pyramidal cells. These type of neurons receive information directly from thalamic neurons and retransmit it to other interneurons or to nearby pyramidal cells. Some non-pyramidal cells have axons oriented horizontally, in the same plane as the cortical layers. An important type of neuron with horizontal axon is the basket cell, which forms dense synaptic connections that envelop the soma of post-synaptic neurons. It is believed that basket cells are responsible for columnar inhibition, which allows neurons in a

cortical column to perform their function relatively independently of that performed by neighboring columns.

1.3 Bioelectric signal transmission

The transmission of the bioelectric signal is the main characteristic of nerve cells (neurons). When a neuron is excited by an external stimuli it becomes the site of an electric field, which propagates along its axon. The electric field consists of a temporary inversion potential at the terminals of the membrane (action potential). The inversion of polarization of the cell is called depolarization, then the potential quickly returns to its rest value of - 90 mV by reconstituting the double layer with negative charges inside and positive charges outside. The arrival of the action potential from an afferent axon causes the depolarization of the presynaptic membrane and that leads, in the chemical synapses, to the opening of the calcium channels (Ca^{2+}). The ions entry induces the fusion of the vesicles with the membrane and the exocytosis of the neurotransmitters contained in them; these cross the synaptic cleft reaching the postsynaptic receptors and this interaction causes the opening of the sodium (Na^+) and potassium (K^+) ionic channels. The ions entry induces the fusion of the vesicles with the membrane and the exocytosis of the contained neurotransmitters; neurotransmitters, through the synaptic cleft, reach the postsynaptic receptors and such interaction causes the opening of the sodium (Na^+) and potassium (K^+) ionic channels. The variation of the intra and extra cellular ionic concentration, producing ionic flows, tends to cancel the membrane potential causing its depolarization (excitatory postsynaptic potential, EPSP). This is not sufficient for generating an action potential: in fact, it is necessary to have several synaptic processes on the same neuron which are close in space and time. The extracellular space around the depolarization will charge negatively with respect to the cellular body and the basal dendrites, which will become

11

electropositive. The resulting electrical field will assume the classical dipolar distribution, with one source corresponding to the electropositive peak, and one sink, corresponding to the electronegative peak (EPSP site). This electrical field will then produce an ions flow in the extracellular space that will create an ionic current, conventionally directed toward the EPSP site (extracellular current). The intracellular space around the depolarization will positively charge itself with respect to the cellular body and the basal dendrites. This imbalance will be compensated by a movement of charges inside the neuron (intracellular currents).

1.4 Stroke: causes, diagnosis and treatment

Stroke is a cerebrovascular lesion caused by the disruption of blood flow to the brain due to an obstruction or rupture of an artery. The interruption deprives the brain of blood and oxygen, causing the death of brain cells.

The human brain consists of more than ten billion cells. These cells require a large amount of energy, in the form of oxygen and glucose. Although the brain represents only 2% of our body weight, it consumes up to 85% of the oxygen we breathe.

When an artery in the brain breaks out or is obstructed, causing blood to stop flowing, the neurons, deprived of the oxygen and nutrients needed for even a few minutes, begin to die. Brain cells destroyed by the initial stroke damage trigger a chain reaction that destroys cells even in a large surrounding area. Because brain cells do not regenerate, stroke damage is often permanent. Depending on which part of the brain is affected by the stroke, the result may be paralysis and loss of speech, vision or memory functions. Stroke can also lead to coma or death. There is a stroke per minute in Western countries.

Strokes are caused by ischaemia or haemorrhage. The ability of the blood to coagulate, while on the one hand it allows the wounds healing, on the other hand it can cause a cerebral ischemia through two distinct processes: embolism and the formation of thrombi. The most common stroke is the thrombotic stroke (cerebral thrombosis). In this type of stroke, a blood clot forms inside a cerebral artery, narrowing the blood vessel. This process can completely interrupt the nutrient supply to the brain area sprayed by the artery that is occluded. In other cases a lump of blood, the embolus, which has formed in another part of the body, usually in the heart, can travel with the blood flow and fix itself in a cerebral artery. If the embolus has a sufficiently large size it can block blood flow to the brain and cause an embolic stroke. Haemorrhagic stroke, which is less frequent but more fatal, is caused by the rupture of a blood vessel in the brain.

Acute stroke therapy aims to achieve the following results:

- The reduction of cerebral edema. Edema is an increase in the volume of the mass present inside the skull as a result of swelling of the nerve cells and/or an increase in the amount of fluid between the nerve cells. In both cases edema behaves like an injury that fills space inside the skull and causes a state of brain suffering. The main drugs that can determine reduction of brain edema are glycerol, mannitol and cortisone;

- The limitation of damage caused by ischaemia. Cerebral ischaemia is the result of a critical imbalance between the metabolic needs of brain tissue (supply of oxygen and glucose) and the ability of the cardiovascular system to meet these needs through adequate blood flow. Accordingly, interventions may consist of: a) reduction of the metabolic needs of the tissue (e.g. hypothermia); b) improving or restoring blood flow.

> Improvements in blood flow may be achieved by raising systemic pressure.

The overall objective of rehabilitation is to contribute to the reduction of disability caused by the patology. The aim of motor rehabilitation is mainly to induce an improvement in the motility levels of the paretic limbs. Numerous studies have highlighted the role of motor rehabilitation at an early stage of the post-ictal course. The first objective is to avoid the most frightening consequences of stroke, i.e. the occurrence of contractures. The second objective consists in facilitating voluntary movements and inhibiting spasticity.

Cognitive rehabilitation aims at the recovery of cognitive functions compromised by stroke. This involves a careful neuropsychological evaluation of the patient by means of a set of tests that explore as extensively as possible the different cognitive functions (language, memory, attentional functions). The aim is to describe a functional profile that allows compromised and conserved abilities to be identified. Rehabilitation techniques can aim at the restoration of the compromised function or at the setting up of strategies that allow to compensate the functional deficit by using saved functions. Particularly encouraging results are being achieved in the application of information technology to cognitive rehabilitation.

1.5 Electromagnetic fields and cortical neurons

The electric field distribution produced by a postsynaptic potential depends on the geometry of the cells, their organization within the cortex and the characteristics of the conductive volume around the active area. As described above, pyramidal neurons are arranged parallel to each other and perpendicularly to the cerebral cortex. Therefore, the simultaneous activation of several pyramidal neurons produces current flows (electric and magnetic fields) which, given their similar orientation, can be added together. The

electric fields generated by pyramidal cells are open fields and therefore, if synchronous, they can accumulate and be registered by means of electrodes placed on the scalp. On the other hand, neuronal structures with elements arranged radially or arranged in random orientations generate closed fields, where intra and extra cellular currents do not produce electric and magnetic fields directed outwards. So, the random orientation of non-pyramidal neurons means that the fields of individual neurons do not add up. In summary, due to their cortical organization and intrinsic structure, the main generators of EEG signals are pyramidal neurons. Electromagnetic fields generated by these neurons are similar to those produced by an electromagnetic dipole, this allows us to describe and model the electromagnetic activity produced by an active cortical area by means of an equivalent dipole.

1.6 From neuronal sources to EEG signal

Generating an EEG signal large enough to be detected requires thousands of cortical neurons activated simultaneously because the contribution of each neuron is extraordinarily small and the signal has to cross several layers of non-neural tissue. Therefore, the amplitude of the recorded signal depends on how synchronized the activity of the involved neurons is. An increase in neuronal activity may occur in different areas of the cortex, and different foci of activity correspond to different distributions of magnetic potential and magnetic flow. The cerebral cortex forms sulci and gyri, and according to the orientation of the active segment (which can be perpendicular or parallel to the scalp) the distribution will be radial or tangent. The dispersion of the potential distribution on the scalp led to the belief that few source points of the brain generate spontaneous EEG phenomena or evoked potentials, and that in practice many EEG spatial patterns could correspond to a few equivalent dipoles (or even just one). But

at the same time, each equivalent dipole could reflect the 'center of mass' of an activity pattern distributed through a region of the skull. The doubts that have arisen have made to face the problem of the spatial focus of the recorded EEG data through the calculation of the surface Laplacian of the potentials, before moving on to the study of the localization of the sources. Laplacian estimation allows a marked reduction in the effects due to the conductive volume and, above all, increases spatial resolution and allows reliable assumptions on brain sources of EEG data (associated with spatial sampling using usually 64-128 electrodes). The idea that only a few sites in the brain are active in generating both evoked and spontaneous EEG potentials has addressed the problem of EEG localization by developing methods that improve spatial resolution without making assumptions about the amount or the distribution of sources in the brain. The potential at the scalp level, due to a single source of current in the brain, is determined by volume conduction of electric fields in a non-homogenous stratified medium. A cortical macro-column (i.e. a hypothetical cylindrical portion of neocortex of longitudinal extension equal to that of the axons remaining within the cortex) of about 3-4 mm diameter contains approximately 10^6 neurons and 10^{10} synapses. The polarization of this volume of tissue is the sum of the micro-sources at the level of the synaptic membranes and other more remote membrane surfaces, and can be approximated as the dipole moment per unit volume. On this spatial scale the cortical tissue seems to show homogeneous statistical properties, but this scale is below the spatial resolution limit of the EEG. The distributed activity through the entire cortex can be represented by many thousands of these dipolar sources, oriented perpendicularly to the cortical surface. The sources in the gyri are mostly radially oriented, while the sources in the sulci are tangentially oriented. The scalp potentials due to radial or tangential dipoles at different depths are represented in Figure 1.4.
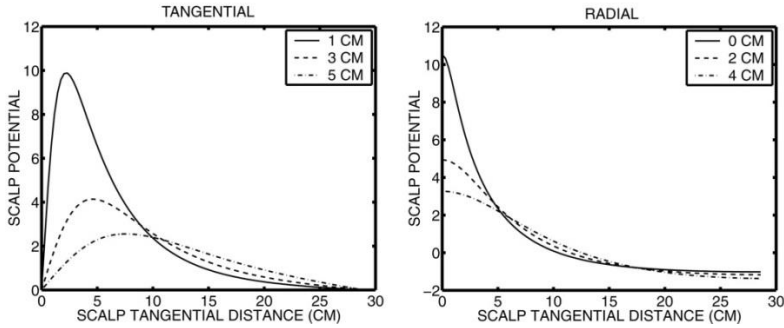
Fig. 1.4 – Trend of scalp potentials due to tangential dipoles (left) and radial dipoles (right).

It is important to underline that the definition of spatial resolution does not coincide with the accuracy of the dipole localization. Spatial resolution is defined as the ability to distinguish two separate dipoles. The resolution is therefore the limit distance, typically the order of magnitude of the distance from the sensor (depth) at which the two dipoles are no longer seen as separate sources. EEG obviously tends to be more sensitive to cortical sources than to deeper sources (which are more distant from the sensors). In addition, the cortical anatomy further amplifies the ability to detect cortical sources since large pyramidal cells are all aligned perpendicularly to the cortical surface. In this way, the measured fields are large because they are produced by the superposition of coherent sources. Deep sources can also be detected, usually by the averaging of many recordings, increasing the signal-to-noise ratio. Note that the EEG is also insensitive to dipoles that are oriented in the opposite direction to the gyri and to random dipoles too (the radial and tangential components elude each other).

1.7 General features of the EEG signal

The EEG is oscillatory in nature. Generally, in the normal human the amplitude of the electric potentials recorded on the scalp varies from 20 to

100 mV. EEG oscillations have frequencies ranging from 1 to 60 Hz. About 90% of the EEG signal seems highly random. These segments often cannot be traced back to particular mental states, are difficult to predict and are usually defined as background activities. The brain is in continuous activity, able to interact and change with the environment, with the other organs of the body and with itself. The EEG traces present a generalized background activity. Small voltage fluctuations of a few tens of microvolts are always present. This spontaneous activity can reveal different mental states, different levels of consciousness or some pathological disorders. This activity is intrinsic to the cerebral matter and its behaviour is an important index of the integrity of the structures and their functionality. Particular waveforms can be good indicators of pathologies, lesions or simply a state of relaxation of the subject. The absence of spontaneous activity is an indication of brain death. Rhythms are categorized basing on the frequency range within which they vary. The various mental and pathological states are often related to oscillations in certain frequency bands, called EEG rhythms, each of which is identified by a letter of the Greek alphabet. The EEG rhythms considered in the basic EEG signal, i.e. detected in the total absence of any exogenous or endogenous stimulus, are classified as described.

Delta rhythms (δ) are oscillations at frequencies below 4 Hz, often of large amplitude, and are a characteristic element of deep sleep and pathological conditions (such as coma states or tumor forms). The theta rhythms (θ) are oscillations in the 4-7 Hz band; in adults they are usually recorded during some states of sleep. Alpha (α) rhythms are included in the 8-13 Hz band and are associated with relaxed wakefulness (best recorded by the parietal and occipital lobes). The desynchronization of the α rhythm, i.e. the decrease in the amplitude of EEG waves in the α band, seems to be related to a greater availability of cortical networks to sensory input or motor control. The rhythms α disappear with the eyes opening. Beta (β) and gamma

(γ) rhythms include all frequencies greater than about 14 Hz (range 14-30 Hz and frequencies greater than 30 Hz, respectively) and are indicative of a state of activation of the cortex (they are usually observed at the level of the frontal areas, but they can also be recorded from other cortical regions). They show the minimum values of their amplitude during intense mental activity. In general, low-frequency and large-amplitude rhythms are associated with sleep phases without dreams or pathological states, while high-frequency and low-amplitude rhythms are associated with alertness and wakefulness or sleep phases with dreams. This is due to the fact that, during deep sleep, cortical neurons are not involved in the processing of information and a large number of them are rhythmically excited by a common, slow and phasic input: in this case the synchrony is high, so the amplitude of EEG potentials is also high. When, on the other hand, the cortex is strongly engaged in processing information, whether it is generated by sensory inputs or internal processes, the level of activity of neurons in large areas of the cortex is relatively high, but this activity is also relatively non-synchronized. In other words, each neuron (or very small group of neurons) is strongly involved in a particular aspect, slightly different from that of the neurons closest to it; the cell, therefore, discharges rapidly, but asynchronously with respect to most of the neighbouring neurons. This poor synchronization results in EEG potentials with modest amplitudes. The various bands show a certain variability individually and with age, it would therefore be preferable to refer to the peak of the α band and define the other bands starting from this peak.

An event, defined as a sensory stimulus or a motor act, can be detected by the analysis of EEG signals, since it mainly creates two types of variations:

- it creates a phase realignment of the signal with respect to the event;
- it creates variations in signal power at different frequencies.

Variations in the EEG are dynamic and of limited duration. The two processes can therefore take place simultaneously and represent only two aspects of the same physiological phenomenon, or they can take place at different times. What interests us is to distinguish physiological phenomena, not the two types of variations. On the other hand, the differentiation in two types of responses depends on the method of analysis used; often they tend to be considered as separate events that are methodologically distinct, but physiologically represent the same phenomenon from two points of view. The best approach to studying brain responses is therefore to study variations in the instants just before or just after the event of interest.

1.8 Electroencephalography

Primary currents, which are sustained by the sum of post-synaptic potentials on the same neuron, affect the synaptic membranes and induce a similar flow of charges in extracellular space: the secondary currents (or volume currents). The latter, flowing through various tissues, reach the surface of the head generating the potential differences measurable by the electrodes placed on the scalp, although strongly attenuated by the low conductivity of these tissues. Most electrodes consist of metal or synthetic ceramic discs or cups. EEG potentials must be measured simultaneously at different points on the scalp. The most commonly used system is the international 10-20 system, in which some anatomical markers (the nasion, the inion and the pre-auricular points A1 and A2) are taken as reference points and 19 electrodes are placed at reciprocal distances equal to 10% and 20% of the distances between these points (Figure. 1.5).
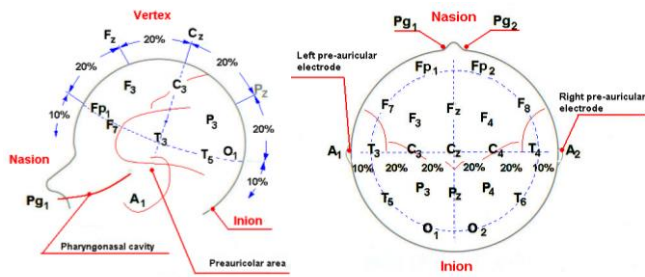
Figure 1.5 - 10-20 system: lateral and upper view.

Since these are potential measurements, one or more reference electrodes must be fixed. The two methods commonly used for this purpose are:

- The common reference method, which measures the potentials of all electrodes against that of a single common electrode, usually placed at the earlobe. The disadvantage of this method is that an activity close to the reference electrode can distort the recording, since it is subtracted from the signals of the other electrodes;

- The average reference method, which refers the value of each channel to the average of all channels. This solves the above problem, but the spatial patterns are smeared.

The study of cortical activity through the analysis of EEG potentials therefore presents a limitation depending on the reference used. Possible variations of the electric potential adopted as reference for the recording of the potentials on the scalp, in fact, can attenuate or obscure some cortical generators, acting, therefore, as a spatio-temporal disturbance factor. Moreover, the potentials recorded on the scalp are not only attenuated, but also distorted and diffused due to the different electrical conductivity of the tissues crossed by the currents. As a result of the spatial distortion phenomena induced by the anatomical structures of the head, the distribution

of potential on the scalp presents a low spatial resolution, which does not allow a reliable localization of the cortical generators of the potentials. Because of these volume conduction effects, the EEG signal is typically a potential that results from overlapping signals from different cortical and subcortical regions. The potential recorded by a certain electrode site, therefore, is not necessarily generated by the underlying cortex: the potential measured on the scalp and generated by bilateral cortical sources may be maximum at the vertex, although this may be far from such sources. It has been quantified, through simulations, that sources distributed within a radius of 3 cm below the electrode position contribute only 50% to the power measured by the electrode itself, while 90% is reached considering sources up to 6 cm away. All in all, the distortion phenomena illustrated produce an increase in the low spatial frequencies of the potentials measured on the scalp (spatial blurring). For all the above reasons, the analysis of spontaneous EEG activity or event-related potentials, performed by means of 20÷30 sensors, generally offers a spatial resolution of about 6÷7 cm, which is at least one order of magnitude worse than those allowed by other commonly used investigation techniques, such as Positron Emission Tomography (PET) or functional Magnetic Resonance Imaging (fMRI). On the other hand, the increase in spatial resolution in the study of EEG potentials cannot be achieved by simply increasing the number of sensors placed on the scalp. In fact, adequate electrodic sampling of the potential on the scalp protects against spatial aliasing phenomena during data acquisition, but does not solve the problem of distortion and attenuation of potential distributions caused by anatomical structures with lower conductivity.

A significant increase in the spatial resolution of the recorded EEG potentials can be obtained by means of the high spatial resolution electroencephalography (HR-EEG): in this case, recordings are made using a network of 64÷128 sensors placed on the scalp and subsequently these data

are processed by special algorithms that remove the attenuation effects induced by low conductivity structures on the head. This last processing step, called spatial deblurring, greatly improves performances when realistic models of conductive volume (obtained by MRI images of the head of the subject under examination) are used.

II

Causality and Influence between Brain Regions

_____

2.1 Introduction

The estimation of the information flow from one area of the cerebral cortex to another is of fundamental importance both in neurological studies and in clinical applications, as it accounts for the propagation of the signal

through the various brain areas during the analyzed experimental task. Since EEG signals are usually characterized by their spectral properties, interest arises in both the direction of the information flow and its spectral content. In order to estimate this flow from the experimental data recorded on the scalp, different methodologies have been used over the years: among others, the Lehmann maps (1987), the Gevins cross-covariance function (1989) or the coherence comparisons as function of the distances between the various electrodes (Thatcher, 1986). Most of these methods, however, have the limit of processing bivariate time series, that is to analyze the relationships between signals taking into account a pair of channels at a time and not the totality of the multi-channel structure. Looking at more than two channels, the complexity of the problem is growing rapidly, which adds to the risk of reaching erroneous conclusions as a result of having partially analyzed the information available. The Partial Directed Coherence method (Baccalá e Sameshima 2001) is a multivariate spectral measurement that can be used to determine the intensity and direction of the information flow between any pair of channels from a single multivariate auto-regressive model (MVAR) estimated over the entire signal set.

2.2 The multivariate auto-regressive model (MVAR)

There are still conflicting opinions in the literature about the linearity and stationarity (in the broad sense) of electroencephalographic signals. Nevertheless, in the following these hypotheses have been assumed to be valid. In particular, it is assumed that an EEG signal, generated by biological events inseparably linked by cause-effect relations, can be modelled through a quasi-stationary process. Furthermore, the analysis of the spectral characteristics of these processes is carried out by means of parametric models.

The model estimation problem is formulated starting from hypotheses that can be imposed on the non-observed part of the realizations, if some characteristics of the signal are 'a priori' known. The parametric spectral estimation is based on two steps:

- definition of a model (i.e. choice of the family of functions with which to characterize the frequency response);

- determination of the parameters of the model.

Once the model has been established, the parameters are determined on the basis of the hypothesis that the observation, represented by N samples of the sequence $\{x(n)\}$, was generated by a white sequence $\{u(n)\}$ (i.e. with impulse autocorrelation). At this point, p coefficients a_1, a_2, ..., a_p characterizing the chosen model, are determined. Based on these, a signal model is generated (which, at this point, can also have an infinite length, or can be large at will), of which the power density spectrum can be calculated. The procedure described above is also illustrated in Figure 2.1.
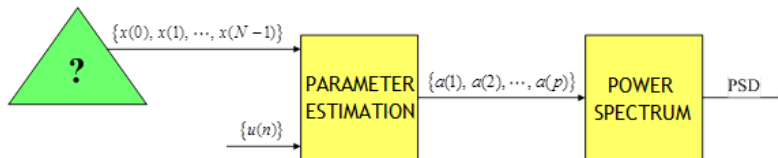
Fig. 2.1 - Parametric spectral estimation.

On the basis of an autoregressive (AR) model, the sample $x(n)$, at the current time n, can be predicted after the parameters $a(k)$ have been estimated, on the basis of its samples extracted at the previous instants $x(n - 1)$, $x(n - 2)$, ..., $x(n - p)$. In bivariate models this principle is applied to two time series. In this way sample $x_1(n)$, extracted from signal $x_1(t)$, can be predicted by including samples extracted, in the previous p samples, from another signal, $x_2(t)$. Similarly, the generic sample $x_2(n)$ can also be predicted on the basis of samples extracted from $x_1(t)$ in the previous p

26

samples. This may be extended to the case where the estimate of $x_1(n)$ takes into account not only the previous p samples of $x_2(t)$, but also the previous p samples of M - 1 signals $x_2(t)$, $x_3(t)$, ..., $x_M(t)$ (Figure 2.2).

The auto-regressive multivariate (MVAR) model of p order, just described, is given by the following equations:

$$x_1(n) = -\sum_{m=1}^{M}\sum_{k=1}^{p} a_{1m}(k)x_m(n-k) + e_1(n)$$

$$x_2(n) = -\sum_{m=1}^{M}\sum_{k=1}^{p} a_{2m}(k)x_m(n-k) + e_2(n)$$

$$\vdots \qquad\qquad \vdots \qquad\qquad \vdots$$

$$x_M(n) = -\sum_{m=1}^{M}\sum_{k=1}^{p} a_{Mm}(k)x_m(n-k) + e_M(n)$$

$$(2.1)$$

where a_{ij} is the auto-regressive parameter relative to the signal pair (i,j), while e_i is the residual (prediction error) relative to the i-th signal.
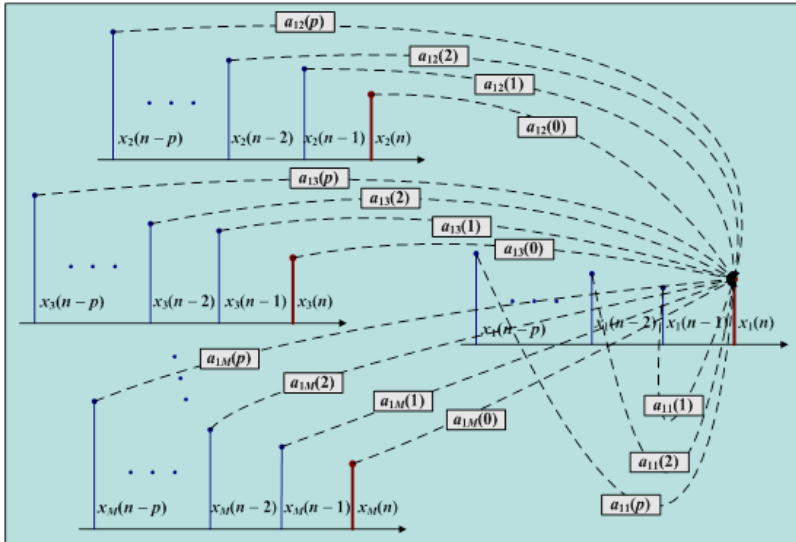
Fig. 2.2 - Connectivity (multivariate case).

The system equations can be represented in the form:

$$\sum_{m=1}^{M}\sum_{k=0}^{p}a_{1m}(k)x_m(n-k)=e_1(n)$$

$$\sum_{m=1}^{M}\sum_{k=0}^{p}a_{2m}(k)x_m(n-k)=e_2(n)$$

$$\vdots \qquad \vdots \qquad \vdots \qquad \bar{a}(0)=\begin{bmatrix}1 & 0 & \cdots & 0\\ 0 & 1 & \cdots & 0\\ \vdots & \vdots & \ddots & \vdots\\ 0 & 0 & \cdots & 1\end{bmatrix}$$

$$\sum_{m=1}^{M}\sum_{k=0}^{p}a_{Mm}(k)x_m(n-k)=e_M(n)$$

(2.2)

For the properties of the Z-transform $\xi(m-m_0)\Rightarrow \Xi(z)z^{-m_0}$, by applying the Z-transform to both members we obtain:

$$\sum_{m=1}^{M}\sum_{k=0}^{p}a_{1m}(k)X_m(z)z^{-k}=E_1(z)$$

$$\sum_{m=1}^{M}\sum_{k=0}^{p}a_{2m}(k)X_m(z)z^{-k}=E_2(z)$$

$$\vdots \qquad \vdots \qquad \vdots$$

$$\sum_{m=1}^{M}\sum_{k=0}^{p}a_{Mm}(k)X_m(z)z^{-k}=E_M(z)$$

(2.3)

In order to move on to the frequency domain f, we remember that $z=e^{j\omega}=e^{j2\pi f/f_s}$, being f_s the rhythm at which the $\chi(n)$ samples are extracted from the $\chi(t)$ waveform. In matrix notation:

$$\bar{A}(f)\bar{X}(f)=\bar{E}(f)$$

(2.4)

where

$$\bar{A}(f) = \begin{bmatrix} A_{11}(f) & A_{12}(f) & \cdots & A_{1M}(f) \\ A_{21}(f) & A_{22}(f) & \cdots & A_{2M}(f) \\ \vdots & \vdots & \ddots & \vdots \\ A_{M1}(f) & A_{M2}(f) & \cdots & A_{MM}(f) \end{bmatrix},$$

$$\bar{X}(f) = \begin{bmatrix} X_1(f) \\ X_2(f) \\ \vdots \\ X_M(f) \end{bmatrix}, \quad \bar{E}(f) = \begin{bmatrix} E_1(f) \\ E_2(f) \\ \vdots \\ E_M(f) \end{bmatrix}$$

(2.5)

The matrix element (i,j) of $\bar{A}(f)$ is the transfer function between the i-th input and the j-th output of the MVAR linear predictor. Generally $A_{ij}(f) \neq A_{ji}(f)$.

The (2.4) can be reformulated as follows:

$$\bar{X}(f) = \bar{A}^{-1}(f)\bar{E}(f) = \bar{H}(f)\bar{E}(f)$$

(2.6)

where $\bar{H}(f)$ is the AR filter transfer matrix, and is defined as

$$\bar{H}(f) = \begin{bmatrix} H_{ii}(f) & H_{ij}(f) \\ H_{ji}(f) & H_{jj}(f) \end{bmatrix}$$

(2.7)

The element (i,j) of the matrix is the transfer function between the i-th input and the j-th output of the MVAR linear predictor. In general $H_{ij} \neq H_{ji}$.

Figure 2.3 shows compact representations of the generator filter and the predictor MVAR.
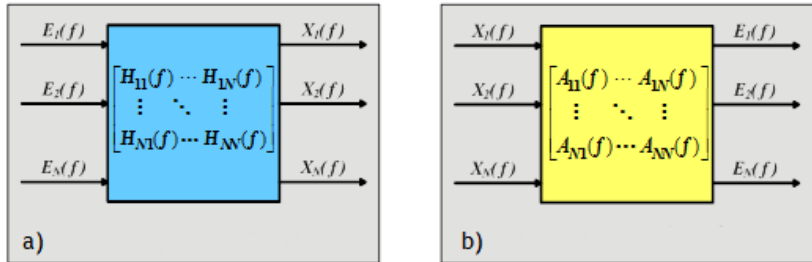
Fig. 2.3 – MVAR a) filter generator and b) linear predictor.

2.3 Selection of the model order

The choice of the auto-regression order in the multivariate models requires a balancing; in fact, if we estimate a too low order MVAR model we risk to neglect relevant information; on the contrary, if we estimate an excessive order model we have a major possibility of prediction error. The order p of the MVAR model is a very important parameter in spectral modelling, because it determines the spectral resolution capacity of the chosen model. In general, a higher order allows for higher spectral resolution, but this may cause the presence of spurious peaks or the splitting of individual peaks in the estimated spectrum. Normally the p order is not known and has to be determined with some criteria. If no knowledge is available a priori, taking into account the equation:

$$\sigma_k^2 = \left(1 + |a_{kk}|^2\right)\sigma_{k-1}^2$$

(2.8)

one can gradually increase the p order until the variance σ_k^2 of the excitation process (decreasing with p), is not decreasing in a way judged negligible (ideally tending to zero).

However, for p values greater than the true order (unknown), there is always a decrease / oscillation of the estimated variance of the excitation process, due to errors in correlation values estimated from the data. In any case, this variance is limited inferiorly by the variance of the real information process of input. Therefore, for a real signal, the choice of the model order is a compromise between spectral resolution and estimation accuracy: a low order means not having a good spectral resolution and an adequate signal description; a high order can improve the resolution, but it increases the variance of the parameter estimation inducing an increase of variance also in the spectrum, with the appearance of spurious peaks (it increases the number of parameters that must be estimated from the same data set). There are criteria for choosing the order of the model, but these

generally tend to underestimate the p order in case of real signals (that are not pure AR processes), but could be well represented with a proper order.

2.3.1 Final Prediction Error

An objective criterion that can be adopted is called the Final Prediction Error (P_{PF}); starting from the prediction error:

$$\varepsilon_p = \sum_{m=0}^{M-1} \left| \sum_{k=0}^{p} a_{pk} x(m-k) \right|^2$$

(2.9)

defines the parameter:

$$P_{PF} = \min_{p} \frac{M+P-1}{M-P-1} \sigma_p^2$$

(2.10)

where m is the number of available samples. In the equation, the variance of the prediction error σ_P^2 decreases with the increasing of p, while the fractional coefficient shows an opposite behavior; it follows that the resulting function has an absolute minimum point.

2.3.2 Akaike Information Criteria

Another index is that provided by the Akaike Information Criteria (Aic):

$$Aic(p) = N \ln(\varepsilon_p) + 2p$$

(2.11)

This criterion defines the optimal value of the p order of the model as the one corresponding to the minimum of this index.

2.3.3 Visual inspection

This method is based on the visualization of the trend in the frequency range of the power density spectrum obtained by the non-parametric method and of the trends obtained by using the parametric methods based on the MVAR model for different values of the p order: the comparison by visual

31

inspection between these trends makes it possible to assess at which value of p the power density spectrum most closely follows the spectrum obtained by the non-parametric method.

2.4 Partial Directed Coherence

Partial Directed Coherence (Baccalá and Sameshima 2001) is a multivariate spectral measurement used to compute the causal influence between signal pairs in a multivariate data set. It has been demonstrated that this estimator is the frequency domain expression of Granger's concept of Causality (Granger, 1969) according to which a time series x[n] influences a second time series y[n] if the knowledge of the 'past' samples of x significantly reduces the prediction error in the estimation of y.

PDC is defined as follows:

$$\pi_{ij}(f) = \left| A_{ij}(f) \right|^2 \tag{2.12}$$

It refers to the MVAR model used as a linear predictor.

However, a normalized version, defined by the following expression, is frequently used:

$$\pi_{ij}(f) = \frac{\left| A_{ij}(f) \right|^2}{\sum_{m=1}^{M} \left| A_{im}(f) \right|^2} \tag{2.13}$$

which can only assume values in the range [0,1]; if $\pi_{ij}(f)=0$, a causal (direct or indirect) influence of x_j on x_i at frequency f can be excluded. We can consider $\pi_{ij}(f)$ as the fraction of the information flowing from node j to node i. The PDC describes the effect of the direct path (i.e. not mediated by any intermediate channel) between j and i. The direct PDC from j to i is related to the fraction of the temporal evolution of the signal i due to the signal j. In the particular case in which j=i, it represents the part of the evolution of the signal relative to the i-th channel that can be explained

exclusively starting from its past, i.e. it represents the auto-regressive part of this signal.

The formulation of the PDC derives directly from the information theory but has been adapted in order to improve the physiological interpretation of the results obtained from electrophysiological data. In particular, a new type of normalization has been introduced, already in use for other connectivity estimators such as the Directed Transfer Function (DTF) (Kaminski and Blinowska, 1991) which consists of dividing each estimated PDC value by the square root of the sum of all elements of the corresponding row (row normalization). The definition becomes as follows:

$$\pi_{ij}^{row}(f) = \frac{A_{ij}(f)}{\sqrt{\sum_{k=1}^{N} A_{ik}(f)A_{ik}^{*}(f)}}$$

(2.14)

In this case the PDC values are between [0;1] too, but obviously the normalization condition changes. Finally, a squared version of the PDC has been introduced (Astolfi et al. 2006) for both types of normalizations. The main difference with the original formulation is, as stated, in the interpretation of these estimators. The quadratic PDC can be related to the power density of the signals and therefore as a fraction of the power density of the i-th signal associated with the j-th measurement. Several simulation studies have highlighted the high performance of this estimator, compared to that of the simple PDC.

2.5 Validation of connectivity estimates

One of the main challenges in the study of brain connectivity based on MVAR modelling is the need to assess the statistical significance of the results obtained. After having obtained the PDC patterns as described in paragraph 2.4 (one for each direction and for each pair of channels), it is

necessary to establish whether the values obtained are statistically significant, i.e. whether they represent the existence of a functional link between the signals or are a purely random values achievable by random oscillations of the signals themselves. This requires a statistical description of the distribution of the PDC values with which to compare the PDC obtained over the relevant period. However, since PDC derives from a strongly non-linear relationship with the time series of the data, its theoretical probability density distribution is unknown. Three methods are used for the statistical validation of connectivity patterns:

- Spectral Causality Criterion;
- Shuffling phases;
- Asymptotic statistics.

The first method consists of applying a threshold value, constant for all frequencies, identified as a white noise threshold, which by definition is considered to be fully uncorrelated. The other two methods are based on building an empirical distribution from surrogate data. These data must verify the hypothesis of null connectivity to allow the construction of a distribution in the case of absence of functional connection. Statistical tests of significance can then be performed on this distribution.

2.5.1 Shuffling phases

The process for constructing the empirical distribution, in the case of shuffling, is as follows: a surrogate data set is generated, dividing the time series of each channel in short periods, and then mixing them randomly and independently, in order to destroy the temporal order. A new model is fitted to the surrogate data, which allows the PDC functions to be computed. Iterating the process, each time on a different set of surrogate data, an empirical distribution of the measures corresponding to null connectivity is created, on the basis of which it is possible to establish a threshold of

significance at the desired level (for example 1%) with which to evaluate the results obtained on the real data. Since the shuffling procedure destroys the temporal structure of the data, for these signals there is no interaction between the channels that can be measured according to the Granger theory (which is based on the temporal order between the signals). The empirical distribution obtained represents the variability of the PDC function under the assumption of no causal relationship.

2.5.2 The Asymptotic statistics procedure

The procedure of asymptotic statistics is based on a recently introduced method (Takahashi et al., 2007), according to which the PDC estimator, in the non-zero case, is consistent and asymptotically normal, while in the null case it tends asymptotically to a χ-square distribution. Therefore, in order to build the empirical distribution, the data collected are forced onto a χ-square distribution using the Monte Carlo method, and the percentile relative to the chosen level of significance is calculated on it. In practice, for the period of interest, the value of the probability distribution is taken; from this distribution is extracted the value corresponding to a percentile of the desired value (i.e. 0.99 for a significance of 0.01), corresponding to the value of the PDC for which the greater values of it have only a 1% probability of occurrence in the case of no connection. This procedure shall be repeated for each frequency sample or frequency band.

2.6 Methods of analysis of complex networks

The information provided by a complex estimator such as the PDC is very extensive: we will have a PDC value for each pair of signals, for each frequency and for each condition. In recent years there has been a need to use indicators to synthetize all this information and make it more accessible. This is why this chapter will be dedicated to graph theory. It was created as a

branch of mathematics and then adapted to the field of neuroscience by defining appropriate indices able to describe a neural network from a local and a global point of view.

The extraordinary brilliance of graphs lies in their simplicity, as they are dots and dashes that unite these dots. But what is really amazing is the power that reflection on these schemes can have.

From the estimation of connectivity patterns associated with EEG activity, brain networks are obtained and their properties can be characterized by graph theory. In fact, the application of this technique makes it possible in general to quantify how communication takes place within complex systems made up of several elements.

2.6.1 Graph definition

A network is a mathematical representation of complex real systems and is defined by a set of nodes (vertices) and arcs (connections).

Different types of graphs can be identified. Graphs in which a unit weight is assigned to each arc (i.e. graphs in which only the existence or absence of connections between different nodes is assessed) are said to be binary or unweighted. A graph is instead defined as weighted when each connection is given a real number representing for example the intensity, length or importance of the arc.

A further classification of graphs can be made on the basis of the directionality property of the arcs. If the arcs indicate only the presence of a relation between two nodes, the graph is defined as undirected; when the arcs also indicate the direction of the influence, highlighting that the activity of one node can depend on the other or vice versa, we refer to it as directed graph.

2.6.2 Extracting the Adjacency Matrix

In the field of neuroscience, graph theory can be used in order to have a better understanding of the organization of the brain network: it is important to define a strategy that allows us to represent neuroanatomic and neurophysiological data in the form of graphs. We can represent the nervous system as a graph considering individual neurons, groups of neurons or specific brain areas as vertices and connections between these elements as arcs. After having represented a cerebral network (or more generally a real network) with a graph, a further step of abstraction can be made by associating a matrix to the graph under examination. In the graph theory, this matrix is defined as an adjacency matrix: it has dimensions N x N (N number of nodes) and the generic element a_{ij} is different from zero if there is a link between nodes i and j. Figure 2.4 shows an example of extraction of the adjacent matrix A from a directional binary graph: the presence of an arc implies elements with a unit weight, while the absence is indicated with null elements ($a_{ij}=0$). If the graph is undirected the adjacent matrix is symmetrical, while it is asymmetrical for the directed graphs.
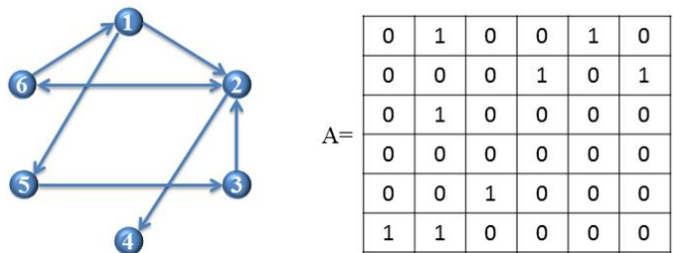
Figure 2.4 - Example of a directed graph with 6 nodes and relative adjacency matrix.

In this study the graph theory is used because it provides an adequate representation of brain networks; in fact the nodes are representative of the electrodes through which the biological signals are acquired, and the arcs

identify the casual relations between the electrodes previously estimated with the theory of connectivity. The method used to obtain the adjacency matrix was to define a threshold value using asymptotic statistics, as described in paragraph 2.5.2 of this chapter. The estimator used for the analysis is based on a multivariate approach, therefore the graph obtained is of a weighted and directed type.

2.6.3 Graph properties

Once the data has been represented with a graph (and its equivalent adjacency matrix), various measures of the graph theory can be performed. A large number of measurements have been developed and can be implemented to characterize complex networks, each of them aimed at describing different network properties. These indices can be grouped into three main categories: measures of centrality, segregation and integration.

The centrality measures the structural and functional importance of each node with respect to the whole network, therefore it concerns measures on the importance of the single node. It is one of the main measures for identifying hubs, nodes that interact with multiple regions. The main centrality measurements are, for example, degree, density and betweenness centrality. Segregation refers to the possibility of the presence of sub-networks and may refer to the existence of specialized areas in the brain where specific processes occur, such as those of response to sensory inputs. An important segregation measure is the clustering ratio. A third category concerns measures which are sensitive to the level of integration of the network. Integration refers to the ability to combine processes distributed in different brain areas, thus the ability of the network as a whole to be interconnected and exchange information. Integration measures include the shortest path or efficiency.

2.6.4 Graph theory indices

The indices are defined from the adjacency matrix derived from a graph. These indices are required to extract synthetic and qualitative information on the network's properties. The following are the simplest, most important and used indices in the field of neuroscience.

2.6.4.1 Network density

The density of a network measures the general connectivity level of the system and is defined as the number of effective arcs L divided by the theoretical maximum number of possible arcs in the graph (Figure 2.5).

$$K = {}^{L}/_{L_{tot}} = {}^{2*L}/_{N(N-1)} \qquad (2.15)$$

where N is the number of nodes and L_{tot} the total number of possible arcs. Density ranges from 0 to 1, the sparser is a graph, the lower is its value.

$$N = 8$$
$$L = 15$$

$$A = \begin{array}{|c|c|c|c|c|c|c|c|}
\hline
0 & 1 & 0 & 0 & 0 & 0 & 1 & 0 \\
\hline
1 & 0 & 0 & 0 & 1 & 1 & 0 & 0 \\
\hline
0 & 1 & 0 & 1 & 0 & 0 & 1 & 0 \\
\hline
0 & 0 & 0 & 0 & 1 & 0 & 0 & 0 \\
\hline
0 & 0 & 0 & 0 & 0 & 0 & 0 & 1 \\
\hline
0 & 0 & 0 & 1 & 1 & 0 & 0 & 0 \\
\hline
0 & 0 & 1 & 0 & 0 & 0 & 0 & 1 \\
\hline
0 & 0 & 0 & 1 & 0 & 0 & 0 & 0 \\
\hline
\end{array}$$

$$k(A) = \frac{15}{56} = 0{,}268$$
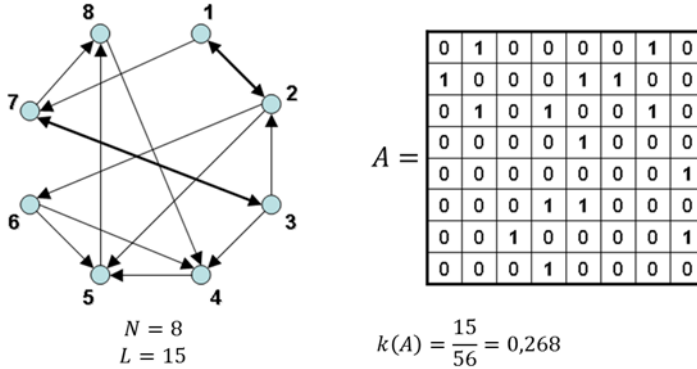
Fig. 2.5 - Example of connection density computation. At the left of the figure, the graph consists of N=8 nodes and L=15 edges. At the right of the figure, the respective adjacency matrix is shown.

2.6.4.2 Node degree

The degree is defined as the total number of arcs connected to a node. In directed networks it is possible to distinguish between in-degree, number of incoming arcs, and out-degree, number of outgoing arcs:

- In-degree, provides the number of connections entering each node:

$$id_i = \sum_j a_{ji} \qquad (2.16)$$

where a_{ji} is the adjacent matrix element that identifies the connection between node i and node j with i,j = 1, ... , N being N the number of vertices of the graph.

- Out-degree, provides the number of outgoing connections from each node:

$$od_i = \sum_j a_{ij} \qquad (2.17)$$

The total degree of node i is therefore given by the following equation:

$$deg_i = id_i + od_i \qquad (2.18)$$

The mean degree of a graph is the mean value of the degree of all the vertices. In the case in which the degree of the node i is null it is defined as isolated node because it is not connected to any vertex of the network. High out-degree values indicate that the node under consideration is a center of emission of information while high in-degree values that the node is common target for most of the other vertexes.

The three indices described above therefore provide us with local network information, node by node. In a weighted graph, the natural generalization of the degree of a node i is the node strength or node weight.

2.6.4.3 Network structure

In a network one is interested in having as much information as possible about the way in which the information transfer takes place; in this context, the geodesic distance between two distinct nodes plays an important role: this quantity identifies the shortest route between the two nodes, i.e. it provides the best path if one wants to make the fastest connection.

The shortest paths of a graph G can be represented through a matrix D whose generic element d_{ij} represents the geodesic distance between nodes i and j. The element of maximum value of this matrix is called diameter of the graph.

Through the D matrix it is possible to define the average length of the shortest paths called path length; this parameter provides a global information of the network and is defined as follows:

$$PL = \frac{1}{N(N-1)} \sum_{i,j} d_{ij} \quad \text{with } i \neq j \tag{2.19}$$

where N is the number of nodes.

The path is therefore a unique sequence of arcs connecting two nodes, and its length is given by the required number of steps (in a binary graph) or by the sum of the lengths of the individual arcs (in a weighed graph). Short Path lengths favour functional integration as they allow communication with a few intermediate steps, minimizing noise effects or information degradation.

It can be noted that in a graph not all nodes are connected to each other and in this case the distance between the two is infinite: in this case the sum of equation 2.19 diverges and it is impossible to obtain a measure for the average geodesic length of the network. To avoid this inconvenience, it is possible to exclude the disconnected node pairs from the calculation or to use an alternative definition which, instead of using the arithmetic mean, calculates the harmonic mean of the geodesic distances.

This second solution has made it possible to define an index known as the global efficiency index E_g, which measures how 'efficient' communication is between all the elements of a network:

$$E_g = \frac{1}{N(N-1)} \sum_{i,j} \frac{1}{d_{ij}} \quad \text{with } i \neq j \tag{2.20}$$

It can be noticed how using the reciprocal geodesics d_{ij} the divergence problem is avoided because the pairs of disconnected nodes give a null contribution.

As the characteristic distance PL, the overall efficiency provides us with a global information of the network being an indicator of the traffic capacity of the same.

Often, however, we are also interested in analyzing the local properties of a graph which can be investigated by considering subgraphs: in fact, for each node i the efficiency of the subgraph can be studied, consisting only of the nodes adjacent to it (two nodes are said to be adjacent if connected by an arc).

A new parameter called local efficiency E_l is therefore introduced, defined as the average of the global efficiencies of all the subgraphs G_i to which the node i does not belong:

$$E_l = \frac{1}{N} \sum_i E_g(G_i) \tag{2.21}$$

This index provides a measure of the system tolerance level for each node when the generic i node is removed, thus showing how efficient communication is between the nodes closest to it.

The clustering coefficient shows the presence of triangles (complete subgraphs of three vertices) in the networks and measures the degree to which the nodes of a graph tend to agglomerate; it is defined as the fraction of triangles around a node compared to the total number of possible triangles, therefore the part of neighbours of a node that are also close to each other. Triangles are important because they are directly linked to the strength of the network.

The clustering coefficient describes the intensity of the interconnections between neighbours of a node. For directed and non-directed graphs we can define, respectively

$$C = \frac{1}{N}\sum_{i\epsilon V}\frac{t_i}{(od_i + id_i)(od_i + id_i - 1) - 2\sum_{j\epsilon V} a_{ij}a_{ji}} \tag{2.22}$$

$$C = \frac{1}{N}\sum_{i\epsilon V}\frac{2t_i}{deg_i(deg_i - 1)} \tag{2.23}$$

where t_i represents the number of triangles related to node i, id_i and od_i are the in-degree and out-degree of node i and a_{ij} the element (i,j) of the adjacency matrix.

By extension, also in the weighed networks it is possible to define the corresponding weighted clustering coefficient, which expresses the relative weight of the neighbours of a node. There are different definitions of this parameter (Saramaki et al. 2007, Barrat et al. 2004, Onnela et al , Zhang and Horvath 2005).

Some parameters, such as clustering coefficients or path lengths, are often normalized by random networks generated with the same number of nodes, arcs, and degrees.

2.6.4.4 Smallworldness

This measure is used to describe the trade-off between local and global integration of a network. A G network is defined as small-world network if $PL_G \sim PL_{rand}$ and $C_G \gg C_{rand}$, where PL_G and C_G represent respectively the path length and the clustering coefficient of the network, while PL_{rand} and C_{rand} the analogous measures in a random graph (Watts and Strogatz 1998). Based on this definition we can express the smallworldness measure of a network like this:

$$S = \frac{C_G/C_{rand}}{PL_G/PL_{rand}} \tag{2.24}$$

A network is defined as small-world if S>1 (Humphries and Gurney 2008).

2.5.5 Random and regular graphs

In graph theory there are two structures that are referenced when studying a real network: random graphs and regular graphs (Figure 2.6).
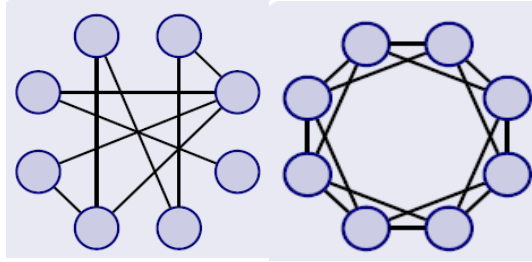
Fig. 2.6 - Examples of random graph (left) and regular graph (right).

These two types of graphs present opposite characteristics: in random graphs the connections between nodes follow a perfectly casual law (high global efficiency and low local efficiency), therefore groups that communicate exclusively with each other and have few connections with the rest of the network are rarely created. In the case of regular graphs each node only communicates with a small number of network vertices that are in its vicinity, so the communication between nodes at a long distance is impaired (low global efficiency and high local efficiency).

Between these two opposite network models, the networks defined as small-world are placed. This measure is used to describe the trade-off between local and global integration of a network. A small-world network is characterized by a shorter path length than a regular network (characterized by high values of clustering and path length) but a greater local interconnectivity than a random network (low values of clustering and path length). Brain networks are characterized by high clustering values and low path length values; this pattern is typical of small-world architecture.

III

Resting state brain connectivity analysis for the characterization of post-stroke patients

3.1 Introduction

Stroke is a pathological cerebral vascular event that causes an acute disturbance of brain function. In Western countries, this disease is the third most common cause of death, after cardiovascular diseases and cancers, and the first absolute cause of disability. Recent epidemiological studies estimate, for the Italian population alone, an incidence of stroke equal to 196,000 new cases every year. About a quarter of stroke sufferers survive with a degree of motor or cognitive disability, sometimes to an extent that makes them unable. At the expense of the acute phase (hospitalization) of

stroke is much higher the cost caused by disability, for the need for hospitalization in care facilities, for the commitment of the family.

Estimation of brain connectivity is a powerful tool for understanding mechanisms underlying integration of activity in different areas of the brain. In recent years, scientific evidence has been presented in cognitive neuroscience regarding the possibility of extracting relevant information about the cognitive state and potential performance of the brain from the mere analysis of activity recorded during the resting state, i.e. when it is not engaged in performing motor or cognitive tasks. In this state, ideally, the only electrical activity in the brain is a spontaneous activity, which can be characterized efficiently by measuring the electroencephalogram at the scalp level. Spontaneous EEG is widely used to assess the general condition of the brain, particularly through the study of the alpha rhythm, which is an index of the level of relaxation of the subject (Greicius et al. 2003). A distinctive property of spontaneous EEG is the 1/f distribution in the spectral domain, so that there is an increase in power towards lower frequencies.

The exigency to study a circumstance in which a subject does not perform any specific task arises from the strong relationship that exists between the spontaneous cerebral activity and the functional connectivity integrity. Most of the studies related to resting state have been conducted in the field of functional Magnetic Resonance Imaging (fMRI). The use of functional magnetic resonance techniques in resting state has in fact provided the possibility of identifying the areas that are activated during the resting state. These include motor and visual networks, two lateral networks (the upper and upper frontal parietal region), the default mode network (formed by the precuneum, frontal medial, lower temporal and lower parietal regions) and a network comprising the insula and anterior cingulate cortex. In particular, among these areas, the default mode network is of great interest, given its strong level of activation during the rest state when

compared to with that observed during task experiments. This suggests the existence of a default state of the brain.

fMRI methodology is characterized by a high spatial resolution, which allows to extract accurate information on the location of the areas involved in the recorded activity, but by a low temporal resolution, which limits the information in the frequency domain and forcing the subject to undergo long acquisition sessions. It is also an expensive examination, not available in all hospitals and not executable on all patients. Methods and equipment are therefore needed to study the spatio-temporal resting state, which can be available in most hospitals and performed on various categories of patients.

The scientific literature relating to the study of resting state in pathological subjects has been increasing greatly in recent years, but in stroke patients it is extremely recent and limited. Most studies in the literature apply graph theory to brain functional networks in order to describe general aspects of communication within these networks (Rubinov and Sporns 2010). In particular, a decrease in local efficiency and an increase in global efficiency compared to the population of healthy are evaluated; another aspect of particular interest concerns alterations in the level of interhemispheric connections in stroke patients (i.e. a decrease in communication between the hemispheres).

Despite the enormous potential, the information provided by these analyses is still not used efficiently in the clinical field because of the difficulty in extracting stable and synthetic indices. Developments aimed at overcoming such limitation could lead to the definition of descriptors that may be related to clinical parameters of interest for the diagnosis, understanding and evaluation of the effects of neuro-rehabilitation therapies.

In such a context, the present study, whose aim is to describe the topographic reorganization after a stroke event of the brain connectivity network related to the resting state condition by various stable and accurate

indexes in a population of stroke patients. Differences in brain network organization are investigated with respect to a healthy population and between different subgroups of patients (subgroups which differ in the side of the lesion) in order to:

- evaluate the deviation from the healthy condition;

- characterize and classify patients on the basis of their clinical features.

3.2 Experimental subjects

The study was conducted on two different populations: twenty-two healthy subjects (mean age 46.1 ± 5.5 years) and forty-two post-stroke patients with mono-lateral lesion (mean age 60.2 ± 12.2 years). For each subject, EEG at resting state was acquired for 120 seconds with closed eyes.

The information available for pathophysiological characterization of clinical features of stroke patients refer to:

- the side of the lesion (i.e. right or left hemisphere lesion);

- severity of injury;

- time since event.

According to the Fugl-Meyer motor scale (FM) patients are classified as severe if FM < 35 and as moderate if FM > 35. Screening was carried out with thirty-six patients in sub-acute phase (within 6 months of the adverse event), and the remaining six in chronic phase (over 6 months). Given the small sample of chronic patients, the study focused on 36 sub-acute subjects: this choice was made in order to ensure greater sample uniformity and eliminate any independent disturbance variable (intervening variable). A first subdivision of the patients group can be made according to one of the parameters describing the pathological state (left/right compared to the injury side).

Given the experimental groups described above, the objectives to be achieved in the present work are:

- to evaluate possible differences between a healthy and a pathological population in the brain networks estimated during resting;

- to characterize the population of stroke patients by assessing the different sub-divisions of patients with respect to the side of the lesion.

To achieve these goals, the analysis was carried out based on a methodological approach oriented to assess and quantify the deviation of patients from the population of healthy (considered as baseline) and any differences between different subgroups.

3.3 Experimental design

For the acquisition of the scalp EEG signal, subjects were required to wear a 64 electrode cuff, which allows them to measure the electrical signals coming from the cortex. Electrode impedances have been kept below 5 KOhms. The software tool that allows the signal to be displayed is the Vision Recorder® which also allows impedance values to be monitored when positioning the electrodes. Out of the 64 channels acquired, 61 represent the acquisition channels, two are the reference channels (relative to the electrodes placed on the earlobes) and one is the ground reference: the acquired signal is therefore the potential difference between each electrode and the reference placed on one of the two lobes.

3.4 Signal processing

After preprocessing – band pass filtering (1-45 Hz), down-sampling at 100 Hz, artifact rejection – the signals were split into one second segments, resulting in 120 trials. In order to reduce the high computational cost of estimating functional connectivity by PDC, the next step in processing was to select a reduced set of channels from which to assess connectivity; the

number of channels was then reduced from 61 to 51. The channels deleted (omitting the most peripheral electrode leads) are Fpz, Af8, Ft8, Tp8, Po8, Oz, Po7, Tp7, Ft7, Af7.

Connectivity estimation has been evaluated using the squared version of the PDC:

$$\pi_{ij}^{S}(f) = \frac{\left|\Lambda_{ij}(f)\right|^2}{\sum_{k=1}^{N}\left|\Lambda_{ik}(f)\right|^2}$$

(3.1)

As previously described in chapter 2 paragraph 2.3, squared PDC can be put in relationship with the power density of the investigated signals and can be interpreted as the fraction of i-th signal power density due to the j-th measure.

Once the connectivity between the considered electrodes had been estimated, it was necessary to apply a statistical validation method in order to distinguish the real connections from those due to random signal fluctuations and measurement errors. Among the methods for the statistical validation of the PDC values described in chapter 2, the asymptotic statistics method was used, which, based on Monte Carlo simulations, makes it possible to obtain a threshold of significance for each pair of channels and each frequency. The validation operation was carried out considering the level of significance 0.05. Since statistical validation was carried out simultaneously on all electrode pairs (N(N-1)) and on all frequencies, it was necessary to consider statistical correction techniques for multiple comparisons in order to avoid the onset of first type errors. In particular, the False Discovery Rate (Benjamini and Yekutieli, 2001) correction was chosen.

Frequency bands of interest were Theta, Alpha, lower Beta, upper Beta and Gamma. To determine the different frequency ranges the Individual Alpha Frequency (IAF) was used, the frequency for which the spectrum in

parieto-occipital electrodes reveals a peak in the Alpha band (Klimesch, 2001). IAF varies both between different subjects and within the same individual as age changes.

The five bands identified for each subject according to the IAF are defined as follows:

- Theta: [IAF-6; IAF-3];
- Alpha: [IAF-2; IAF+2];
- lower Beta: [IAF+3; IAF+11];
- upper Beta: [IAF+12; IAF+20];
- Gamma: [IAF+21; IAF+35].

The population of healthy subjects is characterized by an IAF mean value of 10.25 ± 0.86; the patient population is characterized by an IAF mean value of 9.9 ± 0.74. Statistical comparisons (Student t-tests) were made between the IAF values for the various patient subgroups (regarding the side and/or severity of the injury). No statistically significant differences were found between the various groups, i.e. it can be considered that any observed deviations are due solely to the sampling process.

3.5 Graph theory analysis

Once the connectivity pattern associated with the basic EEG activity of the subjects studied was identified, the brain network of each subject was characterized. For every subject, synthetic indexes were extracted from achieved connectivity patterns; some of them are typical graph-theoretical indices which allow us to describe the general structural complexity of the networks (e.g. clustering, path length), the others were defined and computed in order to underline specific topographic properties (Inter-Hemispheric Connections (IHC) density, asymmetry and influence between hemispheres). These indexes were chosen for the specific pathology in

51

exam: it's known by literature that stroke alters the communication between hemispheres (van Meer et al. 2012).

3.6 Indexes definition

The application of graph theory indices may have limitations in the case of brain network applications. In this case, in fact, one may be interested in aspects that the measures described in chapter 2 cannot describe. However, this limitation can be overcome by defining new indices that capture the properties to be investigated. The following indices are able to evaluate connectivity between and within two sub-areas of a network. These indices are of general impact because they can be applied to any real network by computing them from the matrix of adjacency.

Inter-Hemisferic Connections (IHC)

To evaluate the density of connections between the two hemispheres the implemented index is the Inter-Hemisferic Connections (IHC), defined as:

$$IHC = \frac{L_{SD} - L_{DS}}{L} \qquad (3.2)$$

where L_{SD} and L_{DS} represent respectively the arcs that from the left hemisphere are directed toward the right one and vice versa; L represents the total number of existing arcs.

Asymmetry between hemispheres

In order to obtain a measure of a hemispheric imbalance, the H_SxDx index was defined as follows :

$$H\_S_x D_x = \left(\frac{n\_connS_x}{nTot\_connS_x}\right) - \left(\frac{n\_connD_x}{nTot\_connD_x}\right) \qquad (3.3)$$

where:

- n_connSx is the number of connections in the left hemisphere;
- n_connDx is the number of connections in the right hemisphere;

- nTot_connSx and nTot_connDx represent the total number of possible connections in the left and right hemispheres respectively.

From equation 3.3 it can be seen that the values obtained for H_SxDx vary in the range [-1; 1]. In particular if:

- H_SxDx =1 there are connections only in the left hemisphere (n_connDx = 0) and it is completely connected because the number of existing connections is equal to the total number of possible connections;

- H_SxDx = -1 the situation is the opposite of the one described in the previous point, therefore the imbalance is in favour of the right hemisphere;

- H_SxDx =0, the hemispheres are in symmetry.

Influence between the hemispheres

To evaluate if one of the hemispheres has an effect on the other, the parameter described by the following equation was implemented:

$$I\_S_xD_x = \left(\frac{n\_connS_xD_x - n\_connD_xS_x}{nTot\_connS_xD_x}\right) \tag{3.4}$$

where:

- n_connSxDx is the number of connections that depart from the right hemisphere and terminate in the left hemisphere,

- n_connDxSx are the reverse connections that depart from the left hemisphere and terminate in the right hemisphere

- nTot_connSxDx represents the total number of possible connections connecting one hemisphere to the other.

All indices described here have been calculated for each band, for each subject.

3.7 Statistical analysis

To achieve the proposed objectives, two steps of statistical analysis were performed: one-way ANOVAs performed on each graph indexes with between factor 'subjects' group; a statistical comparison (two-tailed t-tests) between patients' subgroups with indexes measuring asymmetries and influences between the hemispheres. Where the ANOVA was significant, post-hoc tests were performed for multiple comparisons. The post-hoc test used in this study uses the Duncan method.

3.8 Results

Figure 3.3 shows the results of ANOVA performed to investigate the effects of Clustering and IHC indices variations with respect to the factor 'Side of the lesion', in Alpha band. Results demonstrate that, compared with the healthy condition, the values of the two indices decreases significantly in the presence of lesion. There is a statistically significant difference in the density of interhemispheric connections (IHC) between patients with lesion in the left hemisphere and those with lesion in the opposite one; it is worth remembering that all patients are right-handed so their dominant hemisphere is the left one. The left-side lesion group presented worse performance in IHC density: the decrease in interhemispheric density leads to a reduction in post-stroke cerebral plasticity and therefore a lower degree of spontaneous recovery and the need for enhanced rehabilitation training.
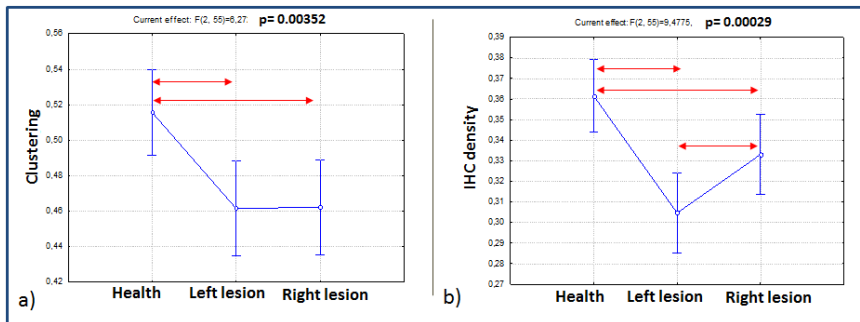
Fig. 3.3 - one-way ANOVA for a) Clustering index and b) Inter-Hemispheric Connections (IHC) density, in Alpha band; "↔" highlights a significant difference (p<0.05)

In figure 3.4 unpaired two tails t-test for Asymmetry and Influence indexes, in the five frequency bands, are shown. In patients an asymmetry between the two hemispheres is observed in the Theta, Alpha and lower Beta bands: the density of connections in the affected hemisphere is greater than in the healthy hemisphere, independently of the side of the lesion. A deviation between the connection densities between the two hemispheres is also observed in terms of Influence in the Alpha and lower Beta bands; furthermore, the connection densities in the affected hemisphere are significantly greater.

A correlation test (Pearson's correlation, significance level 0.05) was performed between the neurophysiological indices that were significantly different between patients with left and right lesions (Figure 3.5a). In order to verify the solidity of the obtained results and to evaluate whether the properties detected by the tests can also be identified at the level of a single subject, a Fisher linear discriminant analysis was used for the classification (Figure 3.5b). The known advantages of the linear discriminant are computational simplicity and easy generalisation (it introduces neither bias nor overfitting, unlike more complex classifiers). As a disadvantage, however, the data must necessarily be separable linearly (not always true in reality), otherwise Fisher's classifier does not come to any result. The leave-

one-out method was used for the classifier training, where the data is divided into training sets (all data minus one) and validation sets (one data, i.e. one patient only). To increase the robustness of the analysis, each subject was classified a number of times using a different training set for each iteration. The variability of the training set was obtained using a smaller number than the available number of subjects in order to obtain a certain number of random combinations. With this procedure, a percentage of iteration classification is obtained for each subject. At the end of these tests, an average of the subjects of the accuracy of the classification shall be made, resulting in an estimate of the degree of data separation.
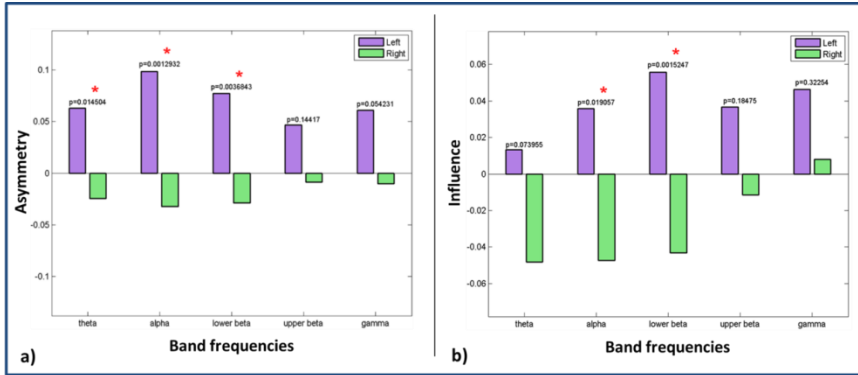
Fig. 3.4 - unpaired two tails t-test for a) Asymmetry and b) Influence indexes, in Theta, Alpha, lower Beta, upper Beta and Gamma bands; "*" highlights a significant difference ($p<0.05$).

Index pairs have been used as features (i.e. features space is two in size). For each band, the classification was made among the patient groups divided on the basis of the site of the lesion.
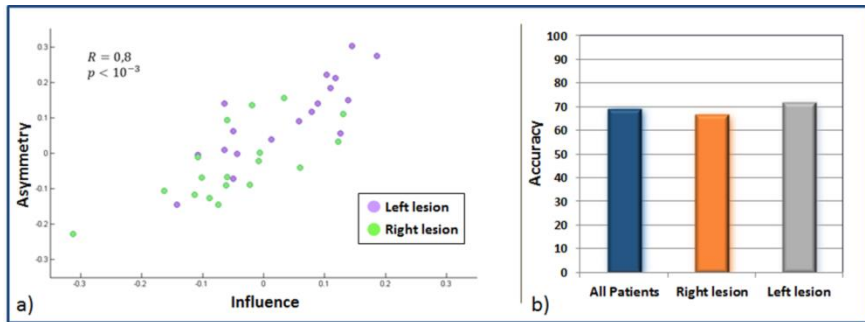
Figure 3.5 - a) Correlation scatter plot and b) Classification accuracy between Asymmetry and Influence indexes for patients, in Alpha band.

3.9 Conclusions

This study was conducted in order to characterize a population of post-stroke patients both in terms of deviation from the condition of the healthy and in terms of statistical differences between sub-groups obtained by determining the side of the injury. This analysis was carried out with an appropriate processing of the EEG data recorded during resting state by advanced signal analysis techniques. After the estimate of the cerebral connectivity made on acquired data, for each subject some synthetic indexes have been computed: some of these indexes are typical of the graph theory and allow to summarize the general properties of the estimated networks, while others have been defined in order to capture particular topographical properties (density of the interhemispheric connections, asymmetries and influences between the hemispheres). The choice of the latter was motivated by the specific pathology as it is known that the stroke causes a reduction in communication between the hemispheres. The obtained results showed that the brain networks of stroke patients at rest are different compared to those of healthy subjects and that the lesion side influence the reorganization after the stroke event. The present study confirms that the protocol used is an adequate tool not only to better understand the pathophysiological

57

mechanisms of the brain, but it's a potentially helpful supplement for diagnostic evaluation and lesions treatments, preparing the ground for future studies aimed to assess the effects of rehabilitative training and to the determination of predictors of recovery after a rehabilitation therapy.

IV

Brain patterns induced by training based on motor imagination assisted by Brain Computer Interface

___

_____

4.1 Introduction

Rehabilitation can be defined as an educational approach aimed at improving the activity and involvement of the subject in the presence of an impairment of functioning due the presence of disabilities, minimizing functional deficits and taking into account environmental and personal factors and existing limitations. Rehabilitation in the hemiplegic patient is aimed at the recovery of the impairment and the optimization of the residual abilities, improving the quality of life through the physical, cognitive, psychological, functional recovery and social relations within the needs of the individual and his family.

Post-stroke functional recovery is sustained by very complex mechanisms that have not yet been fully clarified, but recent studies indicate that rehabilitation interventions can be involved in brain re-organization processes. Among the new technologies applied to rehabilitation, in recent years have been emerging therapies that exploit the possibility of a rehabilitative approach based on the interaction between man and machine, with the possibility of extrapolating precise data useful both for evaluating the tasks performed and for understanding the recovery processes. Identifying the best rehabilitative treatment in this wide context is difficult (Ernst 1990), but rather suggesting an integrated approach with important emerging evidence such as the need to start rehabilitative treatment already in the acute phase, in order to influence the potential of neuroplasticity present in the central nervous system.

Numerous research studies in the literature have shown that the motor imagination of a limb can induce a significant increase in the excitability of the motor cortex and, based on this result, numerous innovative rehabilitation methods have been developed to obtain a specific post-stroke rehabilitation. Mental exercise in the form of motor imaging (Motor Imagery, MI) has long been seen as a cognitive strategy aimed at improving mobility after a stroke (Malouin and Richards 2010). Considerable efforts have been made to improve the nervous mechanisms underlying MI and its relationship with the improvement of sensory-motor regeneration (De Vico Fallani et al. 2013; Kaiser et al. 2012; Sharma and Baron 2013). The reason for using MI in stroke treatment is that the brain's mental practice with a motor content affects those areas of the brain that control movement (Cicinelli et al. 2006; Sharma and Baron 2013). This recurring involvement of motor areas aims to improve brain plasticity and regeneration (Cramer et al. 2011; Dimyan and Cohen 2011). However, the clinical benefits of MI remains doubtful.

The work described in this chapter concerns a study conducted on the electroencephalographic tracks of a group of stroke patients undergoing motor imaging training supported by a Brain Computer Interface (BCI). The objective of the analysis was the data acquired in the second and second-last training session in which the patient performed tasks of motor imagination of the limb whose function had been impaired by stroke. Through advanced, accurate and stable techniques of electroencephalographic signal processing, the study aims to prove and characterize the amount of recovery of patients undergoing rehabilitation training based on motor imagery. During the sessions, the patient's EEG signals were taken and the traces obtained were then processed off-line, until spectral maps of brain activation were obtained. A further contribution is provided by the connectivity estimation through the spectral estimator Partial Directed Coherence (PDC), based on MVAR modelling of acquired electroencephalographic tracks, which has proved to be a powerful tool for the understanding of brain mechanisms based on the integration of activity in different areas of the brain. In this field the graph theory has been widely used to evaluate how the brain communicates between its different regions. Using its many properties, this theory allows the definition of indices that provide useful information on topological properties of complex networks, such as neuronal networks.

In particular, several analyses have been carried out to achieve this objective: 1) to understand if the subjects involved have common cerebral activations, in certain frequency bands, during the performance of the task of motor imagination (closure and extension of the hand); 2) to evaluate a possible improvement, due to training in the motor imagination of the affected limb, using the definition of appropriate spectral indices; 3) to evaluate, through a connectivity study in resting state conditions, whether the organization of the brain affected by the injury presents differences from the organization of the healthy brain hemisphere.

Before starting to describe the rehabilitative approaches used in this work for the rehabilitation of the upper limb, it is important to mention what are the pathophysiological mechanisms that are established as a consequence of a cerebrovascular accident. The two cerebral hemispheres are normally functionally connected through transcallosal connections and are balanced by a mutual interhemispheric inhibition that is altered following a brain injury. Specifically, in the stabilized phase of the disorder, thanks to functional imaging studies, it was possible to investigate the alterations of cortical excitability after stroke by observing a reduced activity of the injured motor cortex, associated with an increased excitability of the intact motor cortex when the patient is asked to move his paretic hand. This condition reflects an over-inhibition of the controlesional hemisphere on the affected hemisphere and may be responsible for an impairment of motor function (Pascual-Leone et al. 2005; Gomez Palacio Schjetnan et al. 2013). It has been shown that this increased activation of the controlesional hemisphere is predominant in patients with poor motor recovery and long-term studies have shown that this hyper-activation decreases over time in relation to functional recovery, so that patients with better motor recovery show a lower activation of the controlesional cortex (Stagg and Johansen-Berg 2013).

The reduced inhibitory activity of the affected hemisphere on the healthy one is justified by the brain lesion and the increased inhibitory activity of the healthy hemisphere can therefore induce an important functional impact as the damaged hemisphere is penalized twice: by the same vascular lesion that damaged it and by the exaggerated transcallosal inhibition. This concept, today widely recognized, goes under the name of 'interhemispheric competition'. The new rehabilitative strategies, therefore, address the recovery of the balance between the two hemispheres in favor of

the affected one, relying on the hypothesis that restoring this disadvantageous condition, can promote the efficiency of motor function.

The meaning of the increased excitability of the healthy hemisphere is still not entirely clear: according to some it represents a direct manifestation of the brain's ability to adapt to an injury and thus to have a role in functional recovery; according to others, it is considered a determining factor in the pathophysiology of the impairment; beyond the reasons given, this excessive inhibition condition is considered decisive in the processes of motor recovery.

4.2 Experimental subjects

The present work aims to study the brain patterns induced in subjects engaged in the execution of a task of motor imagination assisted by Brain Computer Interface (BCI). The task of motor imagination involved the upper limbs, right or left, of subjects with motor difficulties resulting from stroke. Several findings in the literature describe the benefits induced by motor imagination on brain plasticity, and in particular on the responsiveness of the motor cortex (F. Pichiorri et al. 2011). Further studies have shown that the BCI system can perform instantaneous measurements of brain functions modulated by the motor imagination and provide visual feedback to patients, thus resulting in an effective support for post-stroke motor rehabilitation (Floriana Pichiorri et al. 2015).

In this study a group of eighteen subjects was considered. The subjects under examination are post-stroke patients in the sub-acute phase, i.e. within six months of the adverse event, with an average age of 62.6 ± 8.4 years; all subjects present mono-lateral hemispheric lesion (nine with lesion in the right hemisphere and nine with lesion in the left hemisphere). Patients underwent motor imaging training using BCI.

The training protocol includes the recording of EEG tracks during which the patient is required to perform imaginative tasks. The training lasted four weeks, with three sessions per week. Each of the twelve sessions is composed of different runs. Each run involves the recording of a sequence of twenty tasks, in which the subject imagines the movement of the limb corresponding to the affected hemisphere, each alternating with a baseline recording, in which the subject is at rest (resting state). During the task phase, the subject may be asked to imagine a grasping or an extension movement of the hand (Figure 4.1).
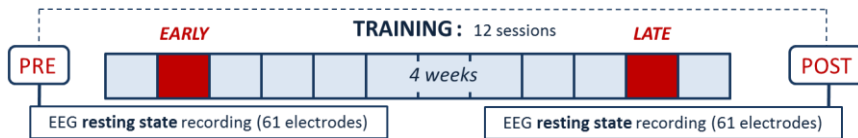
Fig. 4.1 - Rehabilitative protocol.

During BCI training the subject, sitting in a comfortably position in a chair or wheelchair, is covered both forearms with a white cloth. Virtual forearms are projected onto this sheet, designed using an appropriate software (Figure 4.2).

The patient is supported by a therapist, who has a screen in front of him that allows him to continuously monitor the electroencephalographic activity of the patient. The therapist also has a screen showing a cursor and the target zone to be reached. If the patient successfully performs the imagination task, the therapist will see the cursor reach the target and simultaneously the patient will see the virtual hands close or open (feedback to patients in successful trials) depending on the requested task.
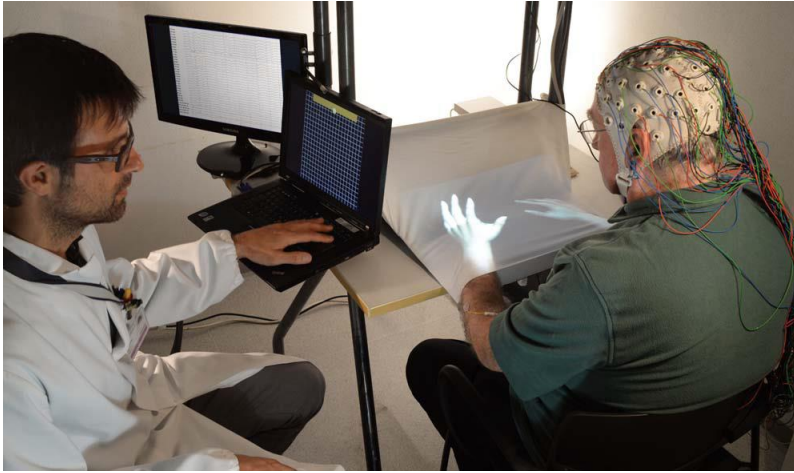
Fig. 4.2 - Prototype setting for the BCI training session.

Each trial begins with a four-second time interval (baseline), during which the patient waits for the command to start the imaginative task. At the end of the baseline, an acoustic signal warns about the beginning of the 'task' phase during which the patient has ten seconds to carry out the imaginative work requested; each run includes twenty trials, each consisting of the baseline and task steps.

For the acquisition of the scalp EEG signal, subjects were required to wear a 64 electrode cuff, which allows them to measure the electrical signals coming from the cortex. Electrode impedances have been kept below 5 KOhms. The software tool that allows the signal to be displayed is the Vision Recorder® which also allows impedance values to be monitored when positioning the electrodes.

In order to assess the BCI training effects, 2 training sessions were analyzed for each subject: an EARLY session, namely the second session for all subjects and a LATE session corresponding to a session in the last week of training, selected according to patient's performance rate. The choice of considering this time interval between training sessions allows statistical comparisons to highlight differences between spectral activations at the start

and end of the training. This allows you to evaluate any improvements made to BCI training.

4.3 Spectral analysis

Spectral analysis was limited to the signals recorded by 31 of the 61 acquisition scalp channels. The 31 selected channels focus on the central area of the scalp (front-central, central, centre-parietal and parietal lines), which is the area of greatest interest in the study of imaginative and motor execution tasks.

After pre-processing - 100 Hz sampling, bandwidth filtering (1-45 Hz), artifact rejection, Common Average Reference (CAR) spatial filtering - the power spectral density (PSD) of the tasks and the underlying EEG signals were calculated using the Welch method (Welch 1967) and averaged over five frequency bands defined according to the individual alpha frequency (IAF):

- Theta (IAF-6; IAF-2);
- Alpha (IAF-2; IAF+2);
- Beta 1 (IAF+2; IAF+11);
- Beta 2 (IAF+11; IAF+20);
- Gamma (IAF+20; IAF+35).

Subjects with lesions in the right hemisphere were flipped in the Left/Right direction in order to consider that the uninjured hemisphere was the right one for all subjects.

In order to highlight the spectral activities associated with the task execution, it was necessary to make a statistical comparison between the power density spectra relative to the baseline data and the tasks associated with each of the thirty-one acquisition channels. The comparison used was the Student T test with a level of significance of 5%. In the case of multiple comparisons, a False Discovery Rate (FDR) correction was chosen. The tests

return negative values of t in the case of desynchronization (i.e. a decrease in power) and positive values of t in the case of synchronization (i.e. an increase in power). In order to obtain an evaluation of the effect of the rehabilitation intervention based on the use of BCI, the second and second to last sessions, respectively EARLY and POST, were considered. Comparisons between EARLY and LATE training sessions were made with a statistical comparison (paired-sample t-test, significance level of 0.05) between negative t-values (associated to the desynchronizations) in the five frequency bands; the significant desynchronizations were obtained from previous statistical comparisons between the task and rest trials.

In the present work specific spectral indices have been used in order to highlight and characterize the activation of the neuroelectric areas involved in a cognitive task and, therefore, to synthesize the results obtained.

4.3.1 Definition of spectral indices

The Global Power Index is defined as the sum of the significant desynchronizations (corresponding to the negative t obtained from the Student test performed between the task and baseline PSDs) detected by the electrodes belonging to the ROI under examination.

$$GlobalPower = \sum_{i=1}^{nD} t_i^-$$ (4.1)

where

nD is the number of desynchronisations;

t_i^- is the i-th desynchronization value.

As expressed in the literature, the choice of negative values of t (desynchronizations), is a good indicator of brain activity elicited by the task of motor imagination to which patients are subjected.

The Mean Power index allows the average brain activation by calculating the average value of all the significant desynchronizations

obtained from the Student T test performed on the Task and Baseline PSDs of an area of interest.

$$MeanPower = \sum_{i=1}^{nD} \frac{\bar{t_i}}{nD} \qquad (4.2)$$

Global and Mean power indices were applied to data obtained from stroke patients in EARLY and LATE sessions to quantitatively determine the desynchronization increase achieved during the MI task. There were calculated for each subject on thirtyone electrodes, every frequency band and session. Then, a statistical comparison (sample pair test, significance level 0.05) was computed.

4.3.2 Results

Figure 4.3 shows the statistical graphs (MI vs. baseline) of a representative patient in the lower beta and alpha bands for the LATE vs EARLY sessions. The color of the pixel codes for the corresponding t-values: green for minor differences, red and blue ranges for significant synchronization or desynchronization. In the EARLY session the pattern in both ranges is two-sided and the t-values are just above the threshold. At a subsequent session, there was greater participation of the affected hemisphere (HA), especially in the lower Beta band. In both frequency bands, spectral desynchronization increased (absolute values were greater than 10), especially in the affected hemisphere.
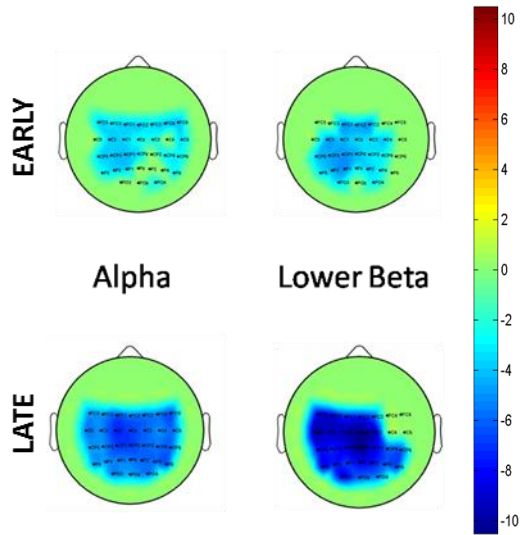
Fig. 4.3 - Statistical scalp maps of a stroke patient: MI vs baseline in Alpha and lower Beta bands for the EARLY and LATE training sessions. Unaffected and Affected Hemisphere (UH; AH) are represented on the right and left of each scalp map, respectively. Color bars code for t-values.

Figure 4.4 shows the results obtained in the group analysis: significant differences were found associated with increased desynchronization only in the Alpha and lower Beta bands. The Alpha band statistical map showed significant activations in FC5, CP5, POz, P2, P4 and PO4, while the lower Beta map showed a large number of statistical differences, especially over the hemisphere where the lesion is: these results show that the desynchronizations associated with the LATE training session are stronger than those associated with the EARLY training session especially in the lower Beta band.
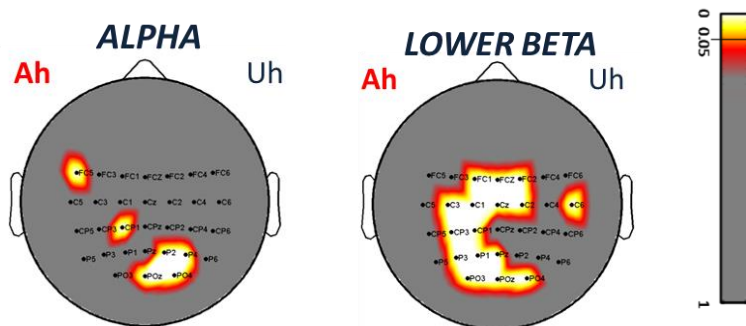
Fig. 4.4 - Maps of p values achieved from the statistical comparison LATE vs EARLY training sessions for BCI patients. The scalp model seen from above with the nose pointing to the upper part of the page, affected hemisphere (ah) is shown on the left side of the. The color of each pixel codes for the correspondent p-value: gray-red for not significant differences, whereas white-yellow for p-values below the threshold.

The results for the Global and Mean power indices for lower Beta band are shown in Figure 4.5: a significant difference has been achieved for both. The other bands behaved the same way. This result revealed a greater commitment to performing the MI at the end of the training session (LATE session).
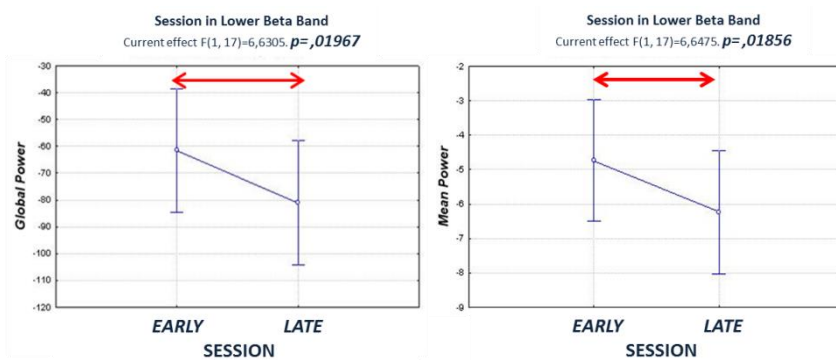
Figure 4.5 – Student t-test for a) Global Power and b) Mean Power, in lower Beta band; "↔" highlights a significant difference (p<0.05)

4.4 Connectivity analysis

In order to highlight changes in the general organization of brain networks between the pre- and post-training phases in resting state a functional connectivity analysis was performed. The study of brain connectivity was performed using the spectral estimator Partial Directed Coherence (PDC) based on MVAR modelling of the electroencephalographic tracks acquired in the baseline phases. In order to reduce the high computational load, the first step required to select a reduced set of channels from which to assess connectivity; the number of channels decreased from 61 to 51. The channels deleted are Fpz, Tp8, Af8, Ft8, Po8, Oz, Tp7, Ft7, Af7, Po7. After preprocessing – band pass filtering (1-45 Hz), down-sampling at 100 Hz, artifact rejection – the signals were split into one second segments. Connectivity estimation has been evaluated using the squared version of the PDC:

$$\pi_{ij}^S(f) = \frac{\left|\Lambda_{ij}(f)\right|^2}{\sum_{k=1}^{N}\left|\Lambda_{ik}(f)\right|^2}$$

(3.1)

The asymptotic statistics method was used as statistical validation method. Frequency bands of interest were Theta, Alpha, lower Beta, upper Beta and Gamma.

For the resting state of each subject, both for the Pre and Post phases, a distribution of PDCs was obtained. The distributions have been achieved through the resampling technique, which consists of considering each time a different sample of one-second trial from which a single PDC is estimated. Once the PDC structures with the dimensions (channels x channels x bands x N resampling) had been obtained, it was possible to perform a statistical comparison, for each subject, between the Pre and Post phases, in order to highlight the significantly different connections.
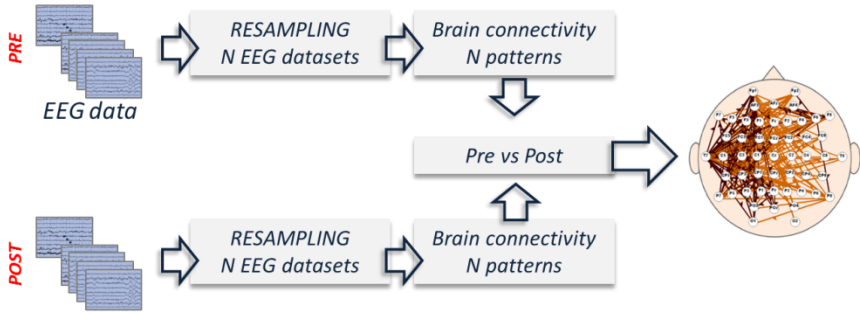
Fig. 4.6 - Steps sequence of resampling technique.

The following parameters have been calculated on the obtained adjacency matrices, obtained for each subject:

- ConnAhUh: describes the number of connections from the lesioned hemisphere to the healthy hemisphere (Ah→Uh);

- ConnUhAh: describes the number of connections from the healthy hemisphere to the lesioned hemisphere (Uh→Ah).

These measures were subjected to an independent two-sample t-test (significance level of 0.05), for each frequency band.

4.4.1 Results

The results of the connectivity analysis are reported in Figure 4.7. Statistical comparisons were made on the indices defined by the structures obtained from the PDC spectral estimator. A significant difference in the ConnAhUh index in the lower Beta band was highlighted: in patients with lesion in the dominant hemisphere, the number of connections from the affected hemisphere (Ah) to the healthy hemisphere (Uh) is significantly higher than in patients with lesion in the right hemisphere.
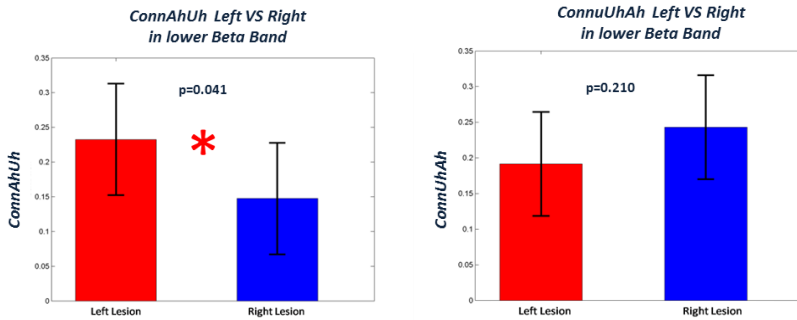
Fig. 4.7 - Student t-test for a) ConnAhUh Index and b) ConnUhAh Index, in lower Beta band; "*" highlights a significant difference (p<0.05)

4.5 Conclusions

The present study on brain-induced patterns in subjects undergoing training of motor imagination supported by brain computer interface, was performed to evaluate the effectiveness of this rehabilitative technique on patients affected by stroke. This analysis was carried out with an appropriate processing of the EEG data recorded during the performance of an experimental task; in particular, the subject was required to imagine a grasping or an extension movement of the hand. The first objective of this study was to understand if the subjects involved have common brain activations in certain frequency bands, during the performance of the motor imagination task. Spectral analysis of EEG signals recorded during the execution of the task with the affected limb showed a higher degree of desynchronization in the LATE session than in the EARLY session. This result, obtained in particular in the Alpha and Lower Beta bands and in specific locations (statistical differences especially above the affected hemisphere), has highlighted an improvement in the execution of the task of motor imagination due to training.

This result was also confirmed by the analysis carried out with appropriate spectral indices. It was shown that subjects with lesion in the

dominant (left) hemisphere generated a greater number of connections from the affected hemisphere to the unaffected hemisphere than subjects with lesion in the non-dominant (right) hemisphere. This is further confirmation of the importance of the dominant hemisphere during motor rehabilitation training. Results of the connectivity analysis were obtained in the lower Beta band which, as reported in the literature, is confirmed to be of considerable importance in the tasks of motor imagination. The results obtained have therefore confirmed not only that the BCI training protocol is an adequate and innovative tool, but have also shown that the methodology developed and applied for the evaluation of this rehabilitative technique is able to provide a measure of the changes induced by the training in communication between the brain areas involved in the execution of the task under investigation.

All the analyses described above lead to similar results and conclusions: increased involvement of the affected hemisphere was observed through training, possibly through the reconstruction of a motor cortex functionality closer to the healthy, as confirmed by the EEG patterns provided by MI under the BCI. It should be explained how this increased motor activity of the brain can affect the functional motor regeneration of patients with subacute disease. Neuroimaging functional brain maps show where cortical activations occur during the task: more interesting results can be obtained by studying how the brain areas involved in the task interact and how this communication is modulated by rehabilitation treatment to investigate plasticity phenomena.

An EEG index of sensorimotor interhemispheric coupling after unilateral stroke

5.1 Introduction

In the physiological conditions, activation of the primary motor cortex (M1) leads to inhibitory effects on the contralater M1, a phenomenon known as interclinical inhibition and reported in detail as altered following a unilateral stroke (Perez and Cohen 2009). As already discussed in section 3.1, the neuroanatomical structure of the interhemispheric inhibition is located in the corpus callosum, the largest brain matter structure whose topographic organization has been widely described (Huang et al. 2005) to reflect the corresponding interconnected cortical areas. Structural and functional changes in interhemispheric coupling after stroke are related to the severity of damage in the corticospinal tract (CST) and therefore to the extent of the motor impairment (Li et al. 2015).

The clinical implications of a stroke are not only related to the effect of the focal lesion, but also to the disruption of connections with other areas (Silasi and Murphy 2014). On the other hand, the interconnected areas contribute to the recovery processes, with both positive and negative effects. Because of these reasons, brain connectivity seems to be a powerful tool for improving the understanding of post-stroke recovery (Grefkes and Fink 2014), as well as to evaluate the extent of damage and the effectiveness of rehabilitation interventions.

Recent studies have shown that interhemispheric connectivity (IHC) in patients with subacute stroke is modulated by several rehabilitation procedures: in particular, a Brain Computer Interface (BCI) motor imagery training of the paretic upper limb in which ipsilesional electroencephalographic sensorimotor rhythms were reinforced, and specifically in the EEG frequency ranges engaged in the training (Pichiorri et al. 2015).

In this study, the aim was to provide an EEG derived IHC index related to the CST integrity and to the severity of the clinical compromise. Motor Evoked Potential (MEP) as evaluated by transcranial magnetic stimulation (TMS) was applied as an indicator of CST integrity and excitability, as an already established predictor of clinical outcome after stroke (Bembenek et al. 2012). To validate the clinical relevance of the identified index, correlations between the index and the motor impairment rate in a population of patients with subacute stroke undergoing rehabilitation have been examined.

5.2 Methods

5.2.1 Patients and corticospinal tract integrity assessment

Thirty stroke patients were consecutively recruited among those hospitalized in our rehabilitation hospital at the Santa Lucia Foundation, IRCCS. The following inclusion criteria were applied: age between 50 and 80 years; first time one-sided stroke (cortical, subcortical or mixed) occurred no more than 6 months prior to inclusion and causing hemiparesis or hemiplegia. At the time of recruitment, patients were evaluated using the European Stroke Scale (ESS; (Hantson et al. 1994)) and the upper limb section of the Fugl-Meyer Assessment (FMA; (Gladstone, Danells, and Black 2002)). The FMA is a functional scale for assessing motor function of the limb; the upper limb section (motor domain) is often used separately and varies from 0 (most affected) to 66 (least affected; (Gladstone, Danells, and Black 2002)). The ESS is a scale of 14 points for evaluating stroke-derived neurological deficits (including motor and non-motor functions), ranging from 0 (most affected) to 100 (least affected; (Lyden and Hantson 1998)).

Transcranial magnetic stimulation (TMS) is a non-invasive and well tolerated technique, widely used in the investigation of the characteristics of excitability and integrity of the central motor tracts in normal subjects and patients with various neurological disorders. Brain stimulation with TMS is achieved by sending pulsing electromagnetic fields from the outside of the head, which induces an electric field onto the brain, causing the neurons to excite. This excitation is obtained by a current pulse transmitted in a coil located on the head of the subject. The waveform of the current that flows in the coil is a sinusoidal pulse, which lasts about 300 milliseconds and has a peak value of 5-10 kA. These pulses cause a coherent neurons activation in the stimulated area, as it happens after the activation related to a synaptic input. The effects that are normally observed after exciting a part of the

cortex with TMS are contracted muscles or phosphenes. In motor cortex stimulation, peripheral effects can be observed by surface electromyography (EMG). In this case the intensity of stimulation used will be that which can activate in the muscles, in a condition of muscle relaxation, a motor evoked potential (MEP) of an amplitude corresponding to that established, according to standard international criteria, for the motor excitability threshold (MT).

The integrity and excitability of the corticospinal tract was determined bilaterally by means of TMS in the following manner. Single-pulse magnetic stimuli were delivered through a round coil on the motor cortex in the optimal position to elicit MEPs in the First Dorsal Interosseus (FDI) muscle. The electromyographic activity (EMG) of FDI was recorded through Ag/AgCl surface electrodes in in a belly-tendon montage.

The raw EMG signal, amplified and bandpass-filtered (0.1 Hz to 2 kHz), was digitized at a sampling frequency of 20 kHz and stored for offline analysis. The integrity of the corticospinal tract was tested at 100% of output stimulator intensity. The presence/absence of an MEP of at least 50 mV was derived from the average of 10 EMG traces. If the MEP was not inducible at rest, the patients were instructed to attempt voluntary contraction.

The presence or absence of MEP relative to the injured side has allowed to divide the sample into two groups, labelled YES and NO respectively. The motor threshold at rest (RMT) was defined as the lowest intensity that produced MEPs greater than 50 mV in at least 5 on 10 consecutive trials in the FDI muscle and was determined bilaterally (affected side, AS and unaffected side, US) in the YES patients and on the unaffected size US only in NO patients. Ten patients had inducible MEPs on the affected FDI muscle (YES).

Statistical comparisons were performed to evaluate differences between YES and NO groups in demographical and clinical characteristics (age, time from event, ESS, FMA), RMT on US (unpaired two-tailed Welch test,

significance level of 0.05). Differences in RMT between AS and US were tested in YES patients (paired t-test, significance level of 0.05). No significant between-group differences were observed for age and time from the stroke event. As expected, the NO group had significantly lower ESS and FMA scores than the YES group ($P < 10^{-6}$ for both ESS and FMA). As for the TMS data analysis, no significant differences in RMT values were observed between groups on US, neither between AS and US in the YES group.

5.2.2 EEG data acquisition and analysis

EEG data were acquired in a separate session (within 1 week from clinical evaluation and TMS assessment). During the EEG data acquisition, patients were comfortably seated in an armchair in a dimly lit room with their upper limbs resting on a desk. Scalp EEG was acquired from 61 standard positions (according to the extended 10–20 International System) band pass–filtered between 0.1 and 70 Hz, digitized at 200 Hz, and amplified by a commercial EEG system.

Five minutes of EEG recordings at rest (eyes closed and relaxed) were acquired. EEG data were down-sampled at 100 Hz and band-pass filtered (1-45 Hz). Artifacts were rejected using a semi-automatic procedure, based on the definition of a voltage threshold (±80 mV). The EEG traces were then segmented into 1 s-epochs and, after relation with the Common Average Reference (CAR), a spectral analysis was performed for all 61 electrodes: at least 100 artefact-free segments were used for each subject for Fast Fourier Transform and power spectral analysis (PSD) in all five frequencies bands of interest. Frequency bands of interest were Theta, Alpha, lower Beta, upper Beta and Gamma whose band limits were defined according to Individual Alpha Frequency (IAF; (Klimesch 1999)). The band filtering parameters were Theta (IAF-6/IAF-2), Alpha (IAF-2/IAF+2), lower Beta

(IAF+2/IAF+11), upper Beta (IAF+11/IAF+20) and Gamma (IAF+20/IAF+35). The IAF range in patients was 9.45 ± 0.54 Hz. To allow a statistical group analysis across all participants, EEG signals were flipped in the Left / Right direction in order to ensure that the lesioned hemisphere was on the left side for all subjects.

To investigate the brain network properties under resting conditions, we estimated the statistical dependencies between EEG data (preprocessed as described above, except for CAR), applying the full multivariate spectral measure Partial Directed Coherence in order to estimate causality in the statistical sense in each patient. The patterns significance against the null case was assessed by means of an asymptotic statistic method (Kaminski et al. 2016) and the obtained estimations were averaged within the five frequency bands as described above.

The neuronal connectivity patterns were analyzed by means of a theoretical graph approach. A new index, called normalized Inter-Hemispheric Strength (nIHS), was defined ad hoc in order to underline the distinctive topographic property of alteration of the communication between hemispheres. It was defined as the sum of weights of interhemispheric links (ihw_i) normalized by the total weight of the network (w_{TOT}):

$$nIHS = \frac{\sum_{i=1}^{N_{IHC}} w_i}{w_{TOT}} \qquad (5.1)$$

where

$$w_{TOT} = \sum_{i=1}^{N} w_i \qquad (5.2)$$

nIHS in (5.1) is the number of non-null interhemispheric links, w_i is the weight of i-th connection and N the total number of connections in the network.

For each patient, nIHS was computed and extracted from the interhemispheric connectivity patterns involving the whole scalp (global nIHS – 44 electrodes) and for those focused in three different subareas (12

electrodes each): a central zone (corresponding to motor and premotor cortices) and occipital and frontal zones, used as control areas (Figure 5.1 for the complete list of electrodes). This subdivision was performed to investigate the possibility to isolate sensorimotor interhemispheric coupling from anterior and posterior areas on the scalp; that is to investigate the macroscopic topographical specificity of the proposed index.

5.2.3 Statistical analysis

To evaluate between-group (YES/NO) differences in the spectral activity at rest, an unpaired two-tailed Welch t-tests between PSD values for each electrode and frequency band was performed. For brain network characteristics, unpaired two-tailed Welch t-tests was computed to identify differences between YES/NO subgroups in the nIHS index for the entire scalp (global) and for each specific area (sensorimotor, frontal and occipital) and EEG frequency band.

A correlation analysis (two-tailed Spearman correlation) between nIHS and clinical scales (ESS and FMA) was performed to further investigate the potential of the proposed effective connectivity index as a neurophysiological descriptor of stroke-derived impairment. In all analysis performed, significance level was set at $P < 0.05$ and False Discovery Rate correction for multiple comparisons was applied to avoid the occurrence of type I errors (Benjamini and Yekutieli 2001).

5.3 Results

No significant differences were observed in the PSD at rest between YES and NO groups, except for the whole scalp PSD in the Theta range of frequency which showed significantly higher value in the NO group (with a prevalence of the affected hemisphere and midline).

The index global nIHS was significantly higher in the YES group in lower beta, higher beta and gamma bands (Figure 5.1a). The same index estimated for the three scalp areas showed significant differences between the YES and NO groups only in the sensorimotor area, in the lower beta band (Figure 5.1b).
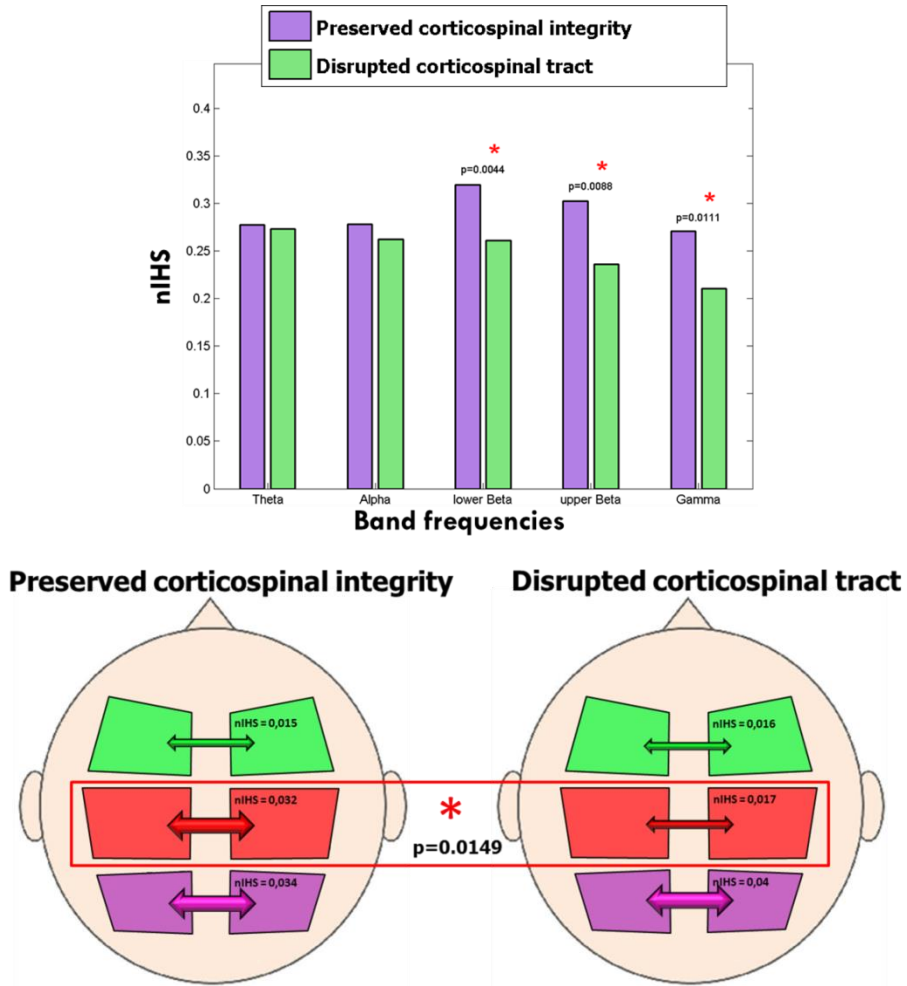
Figure 5.1 – a) Welch t-test for global nIHS statistical comparison between YES and NO groups in the five frequency bands; scalp EEG electrodes used to assess normalized interhemispheric strength in the whole head (global): Fp1-2, Af3-4, F1-2, F3-4, F5-6, F7-8, Fc1-2, Fc3-4, Fc5-6, C1-2, C3-4, C5-6, T7-8, Cp1-2, Cp3-4, Cp5-6, P1-2, P3-4, P5-6, P7-8, Po3-4, O1-2. b) Welch t-test for subgroups nIHS statistical comparison between YES and NO groups in the five frequency bands; scalp EEG electrodes used to assess normalized interhemispheric strength in the three areas: frontal – F1-2, F3-4, F5-6, Fc1-2, Fc3-4, Fc5-6; sensorimotor – C1-2, C3-4, C5-6, Cp1-2, Cp3-4, Cp5-6; occipital – P1-2, P3-4, P5-6, P7-8, Po3-4, O1-2 (colour-coded: green, red and violet, respectively). Statistical significance (p<0.05) is marked by *.

5.4 Discussion

In this study, it was found that CST integrity defined as the presence/absence of MEP induced by TMS in a group of patients with subacute stroke was associated with a significant difference in a defined interhemispheric index derived from EEG analysis. This difference, in favor of the YES group, was specific both from a topographic and a spectral point of view, i.e. it involved scalp electrodes related exclusively to the sensorimotor area and occurred in a range of EEG frequencies associated with movement (lower Beta band).

It was also found that an increase in density of the interhemispheric connections in the YES group affects the overall high frequency EEG spectrum (Beta and Gamma band) when considering the global NIHS index.

This phenomenon is mainly due to the contribution of non-homologous interhemispheric connections in the estimate of the global index. These transversal interconnections are by definition excluded from the calculation of the same index in the three sub-areas of the scalp. Homogeneous networks in the Beta and Gamma frequency bands are in fact an intrinsic part of the entire functional connectivity of the brain at rest (Neuner et al. 2014). Furthermore, the specificity of the IHC value in favour of the YES group is confirmed by the fact that no significant differences were found between the baseline PSD values of the groups in the frequency bands relevant for the IHC differences. In fact, increased power was found only in the slower EEG band (Theta) during resting state in the NO group (especially over the injured hemisphere), a predictable finding in patients with more severe stroke.

The topographical and spectral specificity of NIHS differences as a function of CST integrity makes it plausible that the observed phenomenon reflects a variation at the motor system level. Consistent with previous

findings on hemodynamic neuroimaging (Radlinska et al. 2012), the NIHS index was higher in patients with CST integrity. This index is supposed to reflect and quantify interhemispheric inhibition, which is known to be altered after a stroke at CST level (Perez and Cohen 2009). This hypothesis, however, remains speculative, pending further studies in which observation is not limited to the resting state and includes an extensive neurophysiological evaluations (e.g. TMS measures of intracortical inhibition and facilitation) with stratification of patients according to the size of the stroke lesion (as already done in animal models; (van Meer et al. 2012)).

Compared to other techniques currently used to assess post-stroke connectivity, EEG has some advantages: it is non-invasive, inexpensive, portable and has a high temporal resolution. These advantages are already relevant if we consider connectivity as a possible neurophysiological marker of recovery outcome. However, they become even more precious if one considers the recent approaches in which connectivity itself can be used to guide a neurophysiological design of neurorehabilitation interventions (Silasi and Murphy 2014).

Regardless of the theoretical interpretation of the neurophysiological of the nIHS index, its correlation with the clinical impairment is significant. In the lower beta band the neurosensory nIHS index was positively correlated with the scales of general and upper limb motor impairment, i.e. the higher the nIHS index on the neurosensory areas in the lower Beta band is, the better the clinical and functional motor states measured by the ESS and FMA are.

Objective measures of post-stroke impairment and subsequent recovery are extremely up-to-date in the context of evidence-based neurorehabilitation (Dimyan, Dobkin, and Cohen 2008). Although with caution, we can conclude that our study provides initial evidence for an EEG-based index

which is a measure of the interhemispheric cross-talking and correlates with functional motor impairment in subacute stroke patients. The identified index could be employed to evaluate the effects of training aimed at re-establishing interhemispheric balance and eventually drive the design of future connectivity-driven rehabilitation interventions.

In the context of neurorehabilitation, objective measures of deterioration and post-stroke recovery are evidence-based (Dimyan et al., 2008). We can conclude that this study provides initial evidence for an EEG-based index that is a measure of interhemispheric cross-talking and correlates with functional motor impairment in patients with subacute stroke. The identified index could be used to assess the effects of training to restore interhemispheric balance and ultimately to drive the design of future rehabilitation interventions based on connectivity.

VI

EEG source estimation accuracy in presence of simulated cortical lesions

6.1 Introduction

In the past two decades, there have been major advances in medical imaging, with the development of hard-field imaging methods, such as functional Magnetic Resonance Imaging (fMRI), X-ray Computer Tomography (CT) and Positron Emission Tomography (PET). In spite of their benefits, these methods are all non-portable, expensive and able to image slow metabolic changes over time. The temporal responses of the physiological processes being measured are poor as compared to those of the

electrical signals that define neuronal communication, and recorded signals are only an indirect measure of neural activity. The neural mechanisms at the basis of cerebral dynamics (occurring at faster time-scales) cannot be accurately assessed using these techniques, therefore the resulting mapping of brain functions lacks temporal information about neural activity. Electromagnetic imaging of the brain is the only functional imaging modality that is liable to offer excellent time resolution, recording at the same temporal scale of the dynamic of neural activity. In principle, one could be able to obtain functional images of the brain electrical activity up to every millisecond (which corresponds to the data sampling rate). Electroencephalography (EEG) offers a continuous, real-time, non-invasive measure of brain functioning. This imaging technique is portable, safe, rapid, inexpensive and has an excellent temporal resolution, of the order of milliseconds. For these reasons, although it has a much poorer spatial resolution than the other methods mentioned above, electroencephalography is one of the few techniques allowing to non-invasively study neural activity with a timing that matches the one of the processes under investigation.

EEG measurements are mostly used for diagnostic purposes by direct analysis of signal patterns, but scalp-recorded EEG signals can be also used to calculate the locations of electrical sources in the brain (Michel et al. 2004). Different approaches to localize the sources in the brain have been developed. In basic neuroscience research these tools are used to investigate the functional organization of the human brain and the temporal dynamics of information processing.

It is important to know if a certain change in scalp EEG can be ascribed to the functioning of the brain or if volume conduction effects can cause the observed deviation. Neglecting any of the basic premises underpinning EEG source imaging may result in a localization error or even in the failure of the localization procedure. The localization of brain sources from non-invasive

measurements of electrical or magnetical brain activity is important for both clinical applications and basic brain research. The estimation of the brain sources by means of electroencephalography requires the assumption of (1) a model of possible source positions, (2) an electric forward volume conductor model implementing the electrical and geometrical properties of the solution space, and (3) an inverse source localization method.

Many studies have been performed to quantify the accuracy of the source location via EEG (Akalin Acar and Makeig 2013), even in the presence of brain damage (Bénar and Gotman 2002; Brodbeck et al. 2009; Irimia et al. 2013). In most of these studies, the effects of injuries were assessed by introducing electromagnetic in-homogeneities into the head model and by means of artificial data, i.e. modelling of focal cortical sources. In these simulations: (1) a focal brain activity is simulated in the solution space; (2) the forward solution is calculated to determine the associated EEG distribution; (3) underlying source reconstruction from the potentials in the electrode positions is estimated; (4) localization accuracy is quantified by comparing the simulated and estimated focal source position.

However, a number of problems arise for experimental applications to achieve realistic models that include lesions. The lesions have very variable geometric and electrical properties, therefore individual Magnetic Resonance Images (MRI) and manual segmentation procedures would be required to characterize the pathological tissue, resulting in an additional work that should be justified by a legitimate need and strictly limited to what is necessary. In addition, the electrical properties of brain lesions are variable and often unknown, due to the limited information available. A further divergence of simulation studies from clinical applications is simulated source activity, which is typically composed of one or a few spatially restricted sources, while humans can involve extensive networks of more or less synchronously activated brain areas. EEG data are a superposition of

many effectively independent sources interacting with rhythmic sources of various physiological content. Furthermore, we have to consider that, even applying distributed source imaging, an optimal solution for focal sources could be far from optimality when neurophysiological generators are involved. In fact, the localization error of individual sources cannot predict the performance of an inverse solution in the presence of multiple simultaneously active sources.

As for today, the great deal of uncertainties about the effects of these inhomogeneities for accurate neural source reconstruction preclude the adoption of EEG functional mapping for basic research and clinical applications on patients with brain lesions.

To increase the confidence in source localization procedures and extend their application in pathological subjects, it is important to quantify how the presence of brain lesions affects the distribution of scalp EEG and how to discriminate changes that can be ascribed specifically to the functioning of the brain.

The purpose of this study was to investigate the capability of a distributed source localization method based on the Minimum Norm approach to retrieve extensive sources of activated cortex estimated from actual EEG data by introducing cortical lesions into the generation model. This study was performed in order to specifically quantify the conditions in which source analysis can be performed when anatomical images are not available, and lesion properties cannot be embedded in the head.

For this purpose, the estimated source activity obtained from real data recorded from the scalp potentials was used to simulate different potentials of the scalp EEG (forward problem) and an inverse problem solution was re-computed. The same approach was applied to investigate the effects of the lesion estimation, including 'silent' areas of different sizes in the estimated source activity, but without taking into account any changes in local

conductivities caused by brain injury. The effects of the inclusion of lesions of different sizes and the use of different spatial samplings on the scalp were investigated through statistical analysis, by comparing the error obtained under different conditions.

6.2 Methods

6.2.1 Subjects and Data recording

To generate the simulated data, the first step was to collect real EEG data from 10 healthy subjects (average age 26 ± 2 years; 6 males; all right-handed). All subjects gave their informed consent prior to participation. The high-density EEG recordings were performed by a 61-channel montage (according to an extension of the International 10-20 System) and filtered bandwidth between 0.1 and 70 Hz, digitized at 200 Hz, and amplified by a commercial EEG system. When acquiring EEG data, subjects were comfortably seated on an armchair in a dimly lit room. Five minutes of EEG recordings at rest (relaxed, eyes closed) were acquired. EEG data was filtered bandwidth (1-45 Hz). Artifact rejection was performed using a semi-automatic procedure, based on the definition of a voltage threshold ($\pm$ $80\mu V$).

6.2.2 Estimation of current densities

The electrical neuronal activity that can be measured at the surface of the scalp with the EEG originates mainly from pyramidal cells, located in the grey matter and organized in parallel macro-columns, with an orientation approximately normal to the cortex. These populations can be modeled by a grid of dipole sources located on the cortical surface. The electromagnetic activity produced by an active cortical area is well described and modeled by a single equivalent dipole, thus the electrical and magnetic potentials

generated can be computed at any point in the surrounding space on the condition that a model of the conductive volume is available.

The convoluted anatomy of the cortex was represented using a realistic cortical surface mesh obtained from the anatomical model ICBM152 (Figure 6.1), based on the average of many normal MRI scans (Collins et al. 1999; Fonov et al. 2009). The surface of the cortex was down-sampled to 15,000 vertices. After defining the positions of the dipoles, the orientations were forced to be perpendicular with respect to the cortical surface.
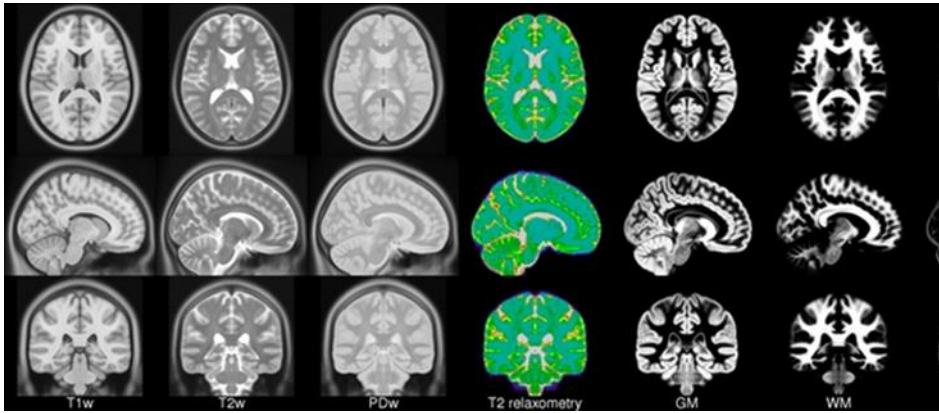
Fig. 6.1 – The Montreal Neurological Institute (MNI) defined a standard brain that is considered representative of the population. MNI152 template is obtained by the average of 152 normal MRI scans.

The forward problem consists in providing the distribution of the electrical potential (or magnetic potential) on a surface that envelops a conductive volume generated by an electromagnetic source localized in the conductive volume itself. In this specific case, the electromagnetic source is represented by the activated cerebral mass, the conductive volume is represented by the head and its structures and the surface that encloses the conductive volume is represented by the scalp. The equations that regulate this problem are the Maxwell equations. The conduction is linear, so the potential on the scalp level due to multiple sources is simply given by the sum of the potentials, each of which originates from each individual source.

The EEG inverse problem is an ill-posed problem since, for all the admissible output voltages, the solution is not univocal (the number of dipoles >> the number of measurements) and unstable (the solution is highly sensitive to the variations of the noisy data). A variety of methods have been described for estimating sources of scalp-recorded electromagnetic activity (Becker et al. 2014; Grech et al. 2008). In this study, the Minimum Norm (MN) solution with Tikhonov regularization was used (Silva et al. 2004). MN solutions are based on the pre assumption that, among all possible source configurations, the source distribution with minimal energy is the most likely.

Given the forward problem

$$X = GS + Y \tag{6.1}$$

where S is the current source, $G \in R^{Nelectrodes \, x \, Ndipoles}$ is the lead field matrix that describes the propagation in the volume conductor and Y is the instrumentation noise, the solution of the optimization problem is:

$$argmin\{\|GS - X\|^2 + \partial\|X\|^2\} \tag{6.2}$$

and $Q = G^T(GG^T + \partial I)^{-1}$ is the Tikhonov regularized inverse matrix of G, where I denotes the identity matrix. In this study the regularization parameter ∂ was estimated by means of the L-curve method (Hansen 2000). In Tikhonov regularization, for the minimization of the least square functional of the reconstruction problem, the regularization consists in adding a penalization function, multiplied by a positive parameter, called regularization parameter ∂, so that the modified function is less sensitive to the noise effect. For small values of the regularization parameter we have a solution that is very sensitive to noise but well reproduces the data; on the contrary, for large values of the regularization parameter we have a solution that is much stable but that badly reproduces the data. In order to find the optimum ∂ value to ensure the best compromise between solution stability and data representation, the criterion of the L-curve was used, consisting of a

parametric curve whose coordinates are the norm of the regularized solution and the corresponding norm residual, obtained for different μ values.

The estimated cortical distributions were used as a basis to generate simulated data with and without the presence of lesions.

6.2.3 Simulation of scalp potentials from cortical activity in absence of lesions

The estimated source activities obtained from each subject were used to simulate the potentials of the EEG scalp (forward problem) in the position of 32 and 64 electrodes uniformly distributed on the surface of the scalp. The equivalent distributed source for the simulated EEG distributions were then calculated using the inverse problem, as the baseline for the study of the simulated lesions.

6.2.4 Simulation of scalp potentials from cortical activity in presence of lesions

The same procedure was performed by including silent lesion areas in the estimated source activity. Before applying forward and inverse problem, the cortical activity of a specific area was reset to zero. We included lesions of two possible dimensions, involving 200 and 1000 dipoles, respectively (Figure 6.2).
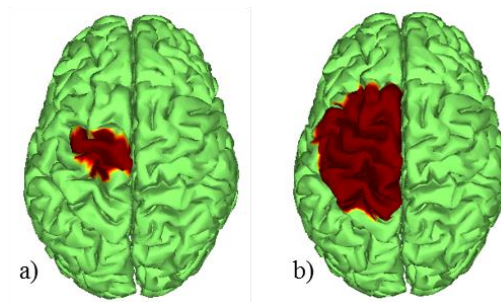
Fig. 6.2 - Cortical model with lesions: a) lesioned area including 200 dipoles; b) lesioned area including 1000 dipoles

6.2.5 Localization errors

For every subject, the cortical activity was estimated from simulated EEG recordings from 32 and 64 electrodes and for the three different conditions of lesion-free, 200-dipoles lesion and 1000-dipoles lesion (Figure 6.3).

For each condition, the error committed in the cortical reconstruction was computed as the difference between the estimated cortical activity and the imposed ones. In particular, to quantify the global accuracy in the whole cortex and the accuracy in the non-lesioned area, we used the normalized Root Norm Square Error (RNSE):

$$RNSE = \frac{\sqrt{\frac{1}{N}}\sqrt{\sum_{i=1}^{N}\|x_i - y_i\|^2}}{\sqrt{\sum_{i=1}^{N}\|x_i\|^2}} * 100 \tag{6.3}$$

where N is the number of dipoles of the whole cortex or of the lesion-free area, x_i and y_i are the activity of dipole $i=1,...,N$ estimated from real and simulated EEG data.
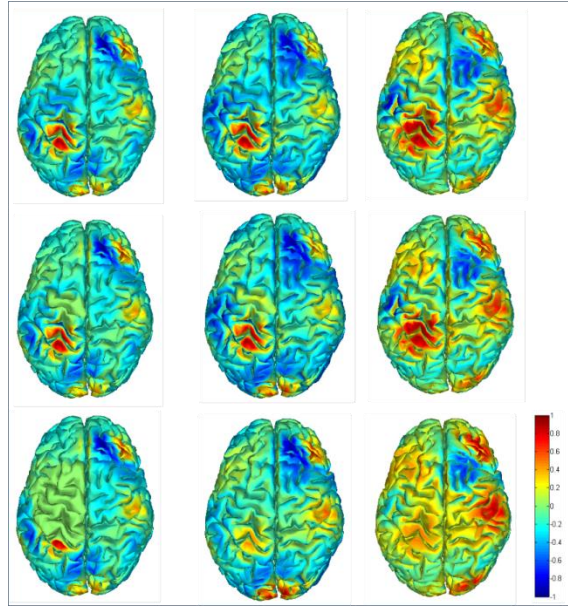
Fig. 6.3 - Cortical activity maps at 2500 ms time point for one subject related to (first column) estimated reference data, (second column) activity reconstructed from 64 electrodes and (third column) from 32 electrodes. The first row is related to the absence of lesions (lesion size=0), the second to a lesion size equal to 200 and the third to a lesion size equal to 1000.

6.3 Statistical Analysis

A statistical analysis of variance (ANOVA) was performed considering as within factors the number of electrodes (two levels: 32 and 64) and lesion size (three levels: 0, 200 and 1000) and as dependent variables the RNSE computed on the whole cortex and on the non-lesioned areas. Significance level was set at $p<0.05$.

6.4 Results

Figure 6.3 shows the activation maps at 2500 ms time point related to simulated reference data (first column), activity reconstructed from 64 electrodes (second column) and from 32 electrodes (third column). The first row is related to the absence of lesions (lesion size=0), the second to a lesion

size equal to 200 and the third to a lesion size equal to 1000. It can be appreciated how the reconstruction is quite accurate when 64 channels are used and deteriorates significantly when we use only 32 channels (He and Musha 1989). The dimension of the lesion also affects the accuracy of the reconstruction.

As for the ANOVA results, Figure 6.4 show the plot of mean for the RNSE error computed on the whole cortex ($F_{(2,18)}=1,8684$; p=0.002) and on the non-lesioned areas ($F_{(2,18)}=2,7124$, p=0.004), respectively. Our results show that both errors are significantly higher, for all lesion dimensions, in the 32 electrodes condition with respect to the 64 electrodes condition. Considering the effect of the lesion dimension, Duncan post-hoc tests returned no significant increase from the lesion-free condition to the 200 dipoles lesion, while a significant increase is reported with respect to the 1000 dipoles lesion. The differences are more evident for the 64 electrodes condition with respect to the 32 electrodes one.
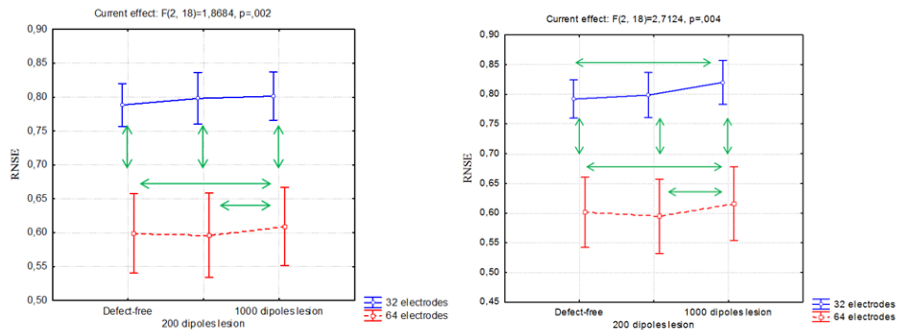
Fig. 6.4 - RNSE error for a) the whole cortex and b) the non-lesioned area. The green arrows indicate a statistically significant difference.

6.5 Conclusion

The aim of this work was to quantify the accuracy of a distributed source localization method in recovering extended sources of activated cortex when cortical lesions of different dimensions are introduced in

simulated data. Methods to reconstruct the neuroelectrical activity in the brain source space can be used to improve the spatial resolution of scalp-recorded EEG and to estimate the locations of electrical sources in the brain. This procedure can improve the investigation of the functional organization of the human brain, exploiting the high temporal resolution of EEG to follow the temporal dynamics of information processing. As for today, the uncertainties about the effects of in-homogeneities due to brain lesions preclude the adoption of EEG functional mapping on patients with lesioned brain.

EEG source-distributed activity estimated from real data was modified including silent lesion areas. Then, for each simulated lesion, forward and inverse calculations were carried out to localize the produced scalp activity and the reconstructed cortical activity. Finally, the error induced in the reconstruction by the presence of the lesion was computed and analyzed in relation to the electrode sampling and to the size of the simulated lesion.

Results returned values of global error in the whole cortex and of error in the non-lesioned area which are strongly dependent from the number of recorded scalp sensors, as they increase when a lower spatial sampling is performed on the scalp (64 versus 32 EEG channels). For increasing sizes of the lesion, statistical analysis showed that only a lesion involving 1000 dipoles induces significantly higher errors level with respect to the lesion-free condition.

The number of sensors of the scalp recorded effect on the accuracy of the reconstruction of the source is a well-known aspect, and explains the reduction of the error due to the increase in the number of electrodes (He and Musha 1989). Due to the generally poorer reconstruction accuracy, the sensitivity of the reconstruction method to the presence of an injury is less evident with 32 electrodes, while when we use 64 electrodes, the accuracy is more influenced by the presence of an injury.

Given the levels adopted in this study, only an injury involving 1000 dipoles induces a significantly higher level of error than the no injury condition.

This study is a preliminary step towards the analysis of the effects of brain injury on the reconstruction of cortical activity distributed by non-invasive scalp data from EEG. The limited experimental sample available here limited statistical analysis to a few factors and levels. Future studies will increase the sample to allow investigation of more factors and levels, such as more electrodes and different lesion positions, in order to quantify the effects of different shape modeling errors in the volume conductor model. This will provide guidelines on the conditions under which a source analysis can be performed without the need to build time/resources consuming cortical injury patterns and those under which such a step is strictly necessary.

Conclusion

Stroke is a very heterogeneous disease, with individuals showing differences in initial clinical condition, in the degree of the spontaneous recovery, and in response to intervention and therapeutic treatment. Indices and predictors for stroke rehabilitation would provide the ability to significantly improve stroke care and management, guiding clinical decision-making, and maximizing opportunities for recovery. Although examinations are conducted using behavioral scales, measurements obtained from neuroimaging of brain function may provide a better characterization of an individual's ability to reorganize neurons than behavioral assessments. As a safe, non-invasive, easy-to-use and inexpensive neuroimage methodology, electroencephalography (EEG) is particularly suitable for measuring and monitoring brain function, particularly in traditionally difficult clinical settings such as stroke. In addition, the EEG provides an excellent temporal resolution for measuring brain activity on a temporal scale close to that of neuronal activity.

This thesis aims to determine the usefulness of EEG measurements in measuring inter-individual differences in brain function, with particular attention to the condition of resting state.

In order to characterize the neuronal properties of patients and to properly evaluate the validity of therapeutic methods, it is necessary to develop indices that express and incorporate the information taken from the recorded signals. Specific characteristics of EEG have been shown to correlate with functional recovery after stroke. In any case, the signal characteristics traditionally used for these purposes are not sufficiently specific and the search for more suitable elements is necessary. In addition to spectral analysis of EEG signals and statistical scalp maps, in this study the

frequency domain Partial Directed Coherence (PDC) technique was used. Since most brain functions involve the coordination of multiple neural areas, measurements that quantify functional connectivity are more advantageous for this purpose than traditional signal analysis techniques. Stroke affects areas of the brain that are distant from the injured ones, but functionally related to them.

Graph theory analysis is increasingly used in the study of structural and functional connectivity of the brain. These factors present a very powerful strategy for understanding the topology and pathology of brain networks due to the high reproducibility and stability of structurally and functionally correlated graphic metrics. However, the confluence of these methods has not yet been fully established. By combining these techniques, this study condensed elaborate matrices of connectivity information into a concise set of clinically useful indices. The physiological interpretations of the measures selected by the graph theory are multiple and quantify the characteristics of different basic mechanisms of motor recovery. We can consider the phases of information processing as increasing levels of abstraction, from measured electrical activity to functional connectivity and network topology measurements. Obviously, the inference of meaning at the level of neurological processes by these graph metrics is essentially an inverse inference, and should be done with great care. On the other hand, differently from behavioural scales, the changes highlighted by these indices may be directly related to changes in functional connectivity measures and in the underlying neuronal activity. Therefore, we focus on their specific association with functional recovery and possible clinical applications.

The first aim of this dissertation was to establish methodology for acquiring and analyzing High Density EEG data. Using a 2 minutes EEG scan acquired at resting state, the first study, after defining indices computed ad hoc to underline specific topographic properties, showed that the brain

networks of stroke patients at rest are different compared to those of healthy subjects and that the lesion side influences the reorganization after the stroke event. In the second study (Chapter 4), prediction of motor improvement with training was found to demonstrate specificity for motor task content. Therefore, these first two studies have shown how interhemispheric connectivity measurements obtained from EEG collected at rest are not only able to characterize the pathology, but also demonstrate the potential of the method to differentiate individuals in order to maximize the response to motor training. In Chapter 5, an EEG-based index related to the CST integrity was defined in order to assess the effects of training to restore interhemispheric balance and ultimately to drive the design of future rehabilitation interventions based on connectivity. The study described in Chapter 6 is a preliminary step in the direction of enabling the adoption of EEG functional mapping after neural source reconstruction also on patients with brain lesions. During my PhD research activity, I implemented a realistic symmetrical finite element head model that allows the presence of four compartments (scalp, skull, brain, lesion). Investigating alterations in the propagation and in the source localization of a simulated realistic lesioned neural activity will increase the confidence in source localization procedures and extend functional connectivity application in pathological subjects.

In summary, the results reported in this dissertation suggest that EEG measures of brain function can be robust predictors of potential reorganization in motor recovery after stroke. Overall, the EEG measures of connectivity have shown particular utility in this respect, overcoming the basic behavioural state and several other clinical measures. The EEG confirms to be a legitimate candidate method for assessing brain function after stroke.

References

Akalin Acar, Zeynep, e Scott Makeig. 2013. «Effects of Forward Model Errors on EEG Source Localization». *Brain Topography* 26 (3): 378–96. https://doi.org/10.1007/s10548-012-0274-6.

Astolfi, Laura, Febo Cincotti, Donatella Mattia, M G Marciani, Luis A Baccalà, Fabrizio de Vico Fallani, Serenella Salinari, Mauro Ursino, Melissa Zavaglia, e Fabio Babiloni. 2006. «Assessing cortical functional connectivity by partial directed coherence: simulations and application to real data». *IEEE Trans Biomed Eng* 53 (9): 1802–1812. https://doi.org/10.1109/TBME.2006.873692.

Baccalá, L. A., e K. Sameshima. 2001. «Partial Directed Coherence: A New Concept in Neural Structure Determination». *Biological Cybernetics* 84 (6): 463–74. https://doi.org/10.1007/PL00007990.

Becker, H., L. Albera, P. Comon, M. Haardt, G. Birot, F. Wendling, M. Gavaret, C. G. Bénar, e I. Merlet. 2014. «EEG Extended Source Localization: Tensor-Based vs. Conventional Methods». *NeuroImage* 96 (agosto): 143–57. https://doi.org/10.1016/j.neuroimage.2014.03.043.

Bembenek, Jan Pawel, Katarzyna Kurczych, Michal Karli Nski, e Anna Czlonkowska. 2012. «The Prognostic Value of Motor-Evoked Potentials in Motor Recovery and Functional Outcome after Stroke − a Systematic Review of the Literature». *Functional Neurology* 27 (2): 79–84.

Bénar, C. G., e J. Gotman. 2002. «Modeling of Post-Surgical Brain and Skull Defects in the EEG Inverse Problem with the Boundary Element Method». *Clinical Neurophysiology: Official Journal of the International Federation of Clinical Neurophysiology* 113 (1): 48–56.

Benjamini, Yoav, e Daniel Yekutieli. 2001. «The Control of the False Discovery Rate in Multiple Testing under Dependency». *The Annals of Statistics* 29 (4): 1165–88. https://doi.org/10.1214/aos/1013699998.

Brodbeck, Verena, Agustina M. Lascano, Laurent Spinelli, Margitta Seeck, e Christoph M. Michel. 2009. «Accuracy of EEG Source Imaging of Epileptic Spikes in Patients with Large Brain Lesions». *Clinical Neurophysiology: Official Journal of the International Federation of Clinical Neurophysiology* 120 (4): 679–85. https://doi.org/10.1016/j.clinph.2009.01.011.

Cicinelli, Paola, Barbara Marconi, Marina Zaccagnini, Patrizio Pasqualetti, Maria Maddalena Filippi, e Paolo Maria Rossini. 2006. «Imagery-

Induced Cortical Excitability Changes in Stroke: A Transcranial Magnetic Stimulation Study». *Cerebral Cortex (New York, N.Y.: 1991)* 16 (2): 247–53. https://doi.org/10.1093/cercor/bhi103.

Collins, D. Louis, Alex P. Zijdenbos, Wim F. C. Baaré, e Alan C. Evans. 1999. «Animal+insect: Improved cortical structure segmentation». In *Ipmi*, 210–223. Springer.

Cramer, Steven C., Mriganka Sur, Bruce H. Dobkin, Charles O'Brien, Terence D. Sanger, John Q. Trojanowski, Judith M. Rumsey, et al. 2011. «Harnessing Neuroplasticity for Clinical Applications». *Brain: A Journal of Neurology* 134 (Pt 6): 1591–1609. https://doi.org/10.1093/brain/awr039.

De Vico Fallani, Fabrizio, Floriana Pichiorri, Giovanni Morone, Marco Molinari, Fabio Babiloni, Febo Cincotti, e Donatella Mattia. 2013. «Multiscale Topological Properties of Functional Brain Networks during Motor Imagery after Stroke». *NeuroImage* 83 (dicembre): 438–49. https://doi.org/10.1016/j.neuroimage.2013.06.039.

Dimyan, Michael A., e Leonardo G. Cohen. 2011. «Neuroplasticity in the Context of Motor Rehabilitation after Stroke». *Nature Reviews. Neurology* 7 (2): 76–85. https://doi.org/10.1038/nrneurol.2010.200.

Dimyan, Michael A., Bruce H. Dobkin, e Leonardo G. Cohen. 2008. «Emerging Subspecialties: Neurorehabilitation». *Neurology* 70 (16): e52–54. https://doi.org/10.1212/01.wnl.0000309216.81257.3f.

Ernst, E. 1990. «A Review of Stroke Rehabilitation and Physiotherapy». *Stroke* 21 (7): 1081–85.

Fonov, VS, AC Evans, RC McKinstry, CR Almli, e DL Collins. 2009. «Unbiased nonlinear average age-appropriate brain templates from birth to adulthood». *NeuroImage* 47 (luglio): S102–S102. https://doi.org/10.1016/s1053-8119(09)70884-5.

Gladstone, David J., Cynthia J. Danells, e Sandra E. Black. 2002. «The Fugl-Meyer Assessment of Motor Recovery after Stroke: A Critical Review of Its Measurement Properties». *Neurorehabilitation and Neural Repair* 16 (3): 232–40. https://doi.org/10.1177/154596802401105171.

Gomez Palacio Schjetnan, Andrea, Jamshid Faraji, Gerlinde A. Metz, Masami Tatsuno, e Artur Luczak. 2013. «Transcranial Direct Current Stimulation in Stroke Rehabilitation: A Review of Recent Advancements». Research article. Stroke Research and Treatment. 2013. https://doi.org/10.1155/2013/170256.

Grech, Roberta, Tracey Cassar, Joseph Muscat, Kenneth P. Camilleri, Simon G. Fabri, Michalis Zervakis, Petros Xanthopoulos, Vangelis Sakkalis, e Bart Vanrumste. 2008. «Review on Solving the Inverse Problem in EEG Source Analysis». *Journal of Neuroengineering*

and Rehabilitation 5 (novembre): 25. https://doi.org/10.1186/1743-0003-5-25.

Grefkes, Christian, e Gereon R. Fink. 2014. «Connectivity-Based Approaches in Stroke and Recovery of Function». *The Lancet. Neurology* 13 (2): 206–16. https://doi.org/10.1016/S1474-4422(13)70264-3.

Greicius, Michael D., Ben Krasnow, Allan L. Reiss, e Vinod Menon. 2003. «Functional Connectivity in the Resting Brain: A Network Analysis of the Default Mode Hypothesis». *Proceedings of the National Academy of Sciences of the United States of America* 100 (1): 253–58. https://doi.org/10.1073/pnas.0135058100.

Hansen, P. C. 2000. «The L-Curve and its Use in the Numerical Treatment of Inverse Problems». In *in Computational Inverse Problems in Electrocardiology, ed. P. Johnston, Advances in Computational Bioengineering*, 119–142. WIT Press.

Hantson, L., W. De Weerdt, J. De Keyser, H. C. Diener, C. Franke, R. Palm, M. Van Orshoven, H. Schoonderwalt, N. De Klippel, e L. Herroelen. 1994. «The European Stroke Scale». *Stroke* 25 (11): 2215–19.

He, B., e T. Musha. 1989. «Effects of Cavities on EEG Dipole Localization and Their Relations with Surface Electrode Positions». *International Journal of Bio-Medical Computing* 24 (4): 269–82.

Huang, Hao, Jiangyang Zhang, Hangyi Jiang, Setsu Wakana, Lidia Poetscher, Michael I. Miller, Peter C. M. van Zijl, Argye E. Hillis, Robert Wytik, e Susumu Mori. 2005. «DTI Tractography Based Parcellation of White Matter: Application to the Mid-Sagittal Morphology of Corpus Callosum». *NeuroImage* 26 (1): 195–205. https://doi.org/10.1016/j.neuroimage.2005.01.019.

Humphries, Mark D., e Kevin Gurney. 2008. «Network "Small-World-Ness": A Quantitative Method for Determining Canonical Network Equivalence». *PloS One* 3 (4): e0002051. https://doi.org/10.1371/journal.pone.0002051.

Irimia, Andrei, S. Y. Matthew Goh, Carinna M. Torgerson, Micah C. Chambers, Ron Kikinis, e John D. Van Horn. 2013. «Forward and Inverse Electroencephalographic Modeling in Health and in Acute Traumatic Brain Injury». *Clinical Neurophysiology: Official Journal of the International Federation of Clinical Neurophysiology* 124 (11): 2129–45. https://doi.org/10.1016/j.clinph.2013.04.336.

Kaiser, Vera, Ian Daly, Floriana Pichiorri, Donatella Mattia, Gernot R. Müller-Putz, e Christa Neuper. 2012. «Relationship between Electrical Brain Responses to Motor Imagery and Motor Impairment in Stroke». *Stroke* 43 (10): 2735–40. https://doi.org/10.1161/STROKEAHA.112.665489.

Kaminski, Maciej, Aneta Brzezicka, Jan Kaminski, e Katarzyna J. Blinowska. 2016. «Measures of Coupling between Neural Populations Based on Granger Causality Principle». *Frontiers in Computational Neuroscience* 10: 114. https://doi.org/10.3389/fncom.2016.00114.

Klimesch, W. 1999. «EEG Alpha and Theta Oscillations Reflect Cognitive and Memory Performance: A Review and Analysis». *Brain Research. Brain Research Reviews* 29 (2–3): 169–95.

Li, Yongxin, Ping Wu, Fanrong Liang, e Wenhua Huang. 2015. «The Microstructural Status of the Corpus Callosum Is Associated with the Degree of Motor Function and Neurological Deficit in Stroke Patients». *PloS One* 10 (4): e0122615. https://doi.org/10.1371/journal.pone.0122615.

Lyden, P. D., e L. Hantson. 1998. «Assessment Scales for the Evaluation of Stroke Patients». *Journal of Stroke and Cerebrovascular Diseases: The Official Journal of National Stroke Association* 7 (2): 113–27.

Malouin, Francine, e Carol L. Richards. 2010. «Mental Practice for Relearning Locomotor Skills». *Physical Therapy* 90 (2): 240–51. https://doi.org/10.2522/ptj.20090029.

Meer, Maurits P. A. van, Willem M. Otte, Kajo van der Marel, Cora H. Nijboer, Annemieke Kavelaars, Jan Willem Berkelbach van der Sprenkel, Max A. Viergever, e Rick M. Dijkhuizen. 2012. «Extent of Bilateral Neuronal Network Reorganization and Functional Recovery in Relation to Stroke Severity». *The Journal of Neuroscience: The Official Journal of the Society for Neuroscience* 32 (13): 4495–4507. https://doi.org/10.1523/JNEUROSCI.3662-11.2012.

Michel, Christoph M., Micah M. Murray, Göran Lantz, Sara Gonzalez, Laurent Spinelli, e Rolando Grave de Peralta. 2004. «EEG Source Imaging». *Clinical Neurophysiology* 115 (10): 2195–2222. https://doi.org/10.1016/j.clinph.2004.06.001.

Neuner, Irene, Jorge Arrubla, Cornelius J. Werner, Konrad Hitz, Frank Boers, Wolfram Kawohl, e N. Jon Shah. 2014. «The Default Mode Network and EEG Regional Spectral Power: A Simultaneous FMRI-EEG Study». *PloS One* 9 (2): e88214. https://doi.org/10.1371/journal.pone.0088214.

Pascual-Leone, Alvaro, Amir Amedi, Felipe Fregni, e Lotfi B. Merabet. 2005. «The Plastic Human Brain Cortex». *Annual Review of Neuroscience* 28: 377–401. https://doi.org/10.1146/annurev.neuro.27.070203.144216.

Perez, Monica A, e Leonardo G Cohen. 2009. «Interhemispheric inhibition between primary motor cortices: what have we learned?» *The*

Journal of Physiology 587 (Pt 4): 725–26. https://doi.org/10.1113/jphysiol.2008.166926.

Pichiorri, F., F. De Vico Fallani, F. Cincotti, F. Babiloni, M. Molinari, S. C. Kleih, C. Neuper, A. Kübler, e D. Mattia. 2011. «Sensorimotor Rhythm-Based Brain-Computer Interface Training: The Impact on Motor Cortical Responsiveness». *Journal of Neural Engineering* 8 (2): 025020. https://doi.org/10.1088/1741-2560/8/2/025020.

Pichiorri, Floriana, Giovanni Morone, Manuela Petti, Jlenia Toppi, Iolanda Pisotta, Marco Molinari, Stefano Paolucci, et al. 2015. «Brain-Computer Interface Boosts Motor Imagery Practice during Stroke Recovery». *Annals of Neurology* 77 (5): 851–65. https://doi.org/10.1002/ana.24390.

Radlinska, Basia A., Yasmin Blunk, Ilana R. Leppert, Jeffrey Minuk, G. Bruce Pike, e Alexander Thiel. 2012. «Changes in Callosal Motor Fiber Integrity after Subcortical Stroke of the Pyramidal Tract». *Journal of Cerebral Blood Flow and Metabolism: Official Journal of the International Society of Cerebral Blood Flow and Metabolism* 32 (8): 1515–24. https://doi.org/10.1038/jcbfm.2012.37.

Rubinov, Mikail, e Olaf Sporns. 2010. «Complex Network Measures of Brain Connectivity: Uses and Interpretations». *NeuroImage* 52 (3): 1059–69. https://doi.org/10.1016/j.neuroimage.2009.10.003.

Sharma, Nikhil, e Jean-Claude Baron. 2013. «Does Motor Imagery Share Neural Networks with Executed Movement: A Multivariate FMRI Analysis». *Frontiers in Human Neuroscience* 7: 564. https://doi.org/10.3389/fnhum.2013.00564.

Silasi, Gergely, e Timothy H. Murphy. 2014. «Stroke and the Connectome: How Connectivity Guides Therapeutic Intervention». *Neuron* 83 (6): 1354–68. https://doi.org/10.1016/j.neuron.2014.08.052.

Silva, C., J. C. Maltez, E. Trindade, A. Arriaga, e E. Ducla-Soares. 2004. «Evaluation of L1 and L2 Minimum Norm Performances on EEG Localizations». *Clinical Neurophysiology: Official Journal of the International Federation of Clinical Neurophysiology* 115 (7): 1657–68. https://doi.org/10.1016/j.clinph.2004.02.009.

Stagg, Charlotte J., e Heidi Johansen-Berg. 2013. «Studying the Effects of Transcranial Direct-Current Stimulation in Stroke Recovery Using Magnetic Resonance Imaging». *Frontiers in Human Neuroscience* 7 (dicembre). https://doi.org/10.3389/fnhum.2013.00857.

Watts, D. J., e S. H. Strogatz. 1998. «Collective Dynamics of "small-World" Networks». *Nature* 393 (6684): 440–42. https://doi.org/10.1038/30918.

Welch, P. D. 1967. «The Use of Fast Fourier Transform for the Estimation of Power Spectra: A Method Based on Time Averaging Over Short,

Modified Periodograms». *IEEE Trans. Audio & Electroacoust., Volume AU-15, p. 70-73* 15: 70–73.

Curriculum vitae

Personal information

First name / Surname: Stefano Caschera

Address: Via Fortebraccio 16, 00176, Roma, ITALY

Telephone Mobile: +39 334 2460371

E-mail: caschera@dis.uniroma1.it

Nationality: Italian

Date of birth: 06 December 1986

Gender: Male

Work experience & education

Dates: 2014 – 2018

Title of qualification: PhD in BioEngineering

Dates: 2012 – 2014

Title of qualification: Master degree in Biomedical Engineering

Experimental Thesis Title:

Resting state brain connectivity analysis aimed to characterize the response to motor rehabilitation of post-stroke patients

Laboratory supervised by: Dr. Donatella Mattia/Prof. Febo Cincotti

Mark of: 110/110

University: "Sapienza" University of Rome, Rome

Dates: 2005 – 2011

Title of qualification: Bachelor in Clinical Engineering

Experimental Thesis Title:

Tomographic reconstruction of cerebral activity from EEG recordings during modulation of mental states

Laboratory supervised by: Prof. Serenella Salinari

University: "Sapienza" University of Rome, Rome

Awards

- Award for best master thesis on Disability theme, Sapienza University of Rome, 2014.
- Thesis award in Biomedical Signal Processing and Imaging, Bioengineering National Group, Bressanone, 2014.

Activities: conferences, courses, seminars and schools

Courses

- Advances in Bioengineering: Auto-regressive methods for biomedical signal processing, Sapienza University of Rome;
- Advances in Bioengineering: Statistical processing of biomedical data, Sapienza University of Rome;
- Advances in Systems and Control: Decidability of robot manipulation planning, Sapienza University of Rome.

Seminars

- Introduction to computational inverse problems, Sapienza University of Rome;
- Technical-scientific writing course, Sapienza University of Rome;
- Math and Brain, Sapienza University of Rome;
- Great Ideas in ICT - Hyperscanning: a new approach to the study of the physiological basis of human social interaction, Sapienza University of Rome;
- The Virtual Brain node 5, Aix-Marseille Université;
- International Workshop on Artificial Intelligence and Cognition, University of Palermo and ICAR-CNR.

Schools

- 9th IEEE-EMBS International Summer School on Biomedical Signal Processing-Biomedical Signal Processing in Neuroengineering: enabling technologies for rehabilitation, University of Pavia;
- XXXV Annual School of Bioengineering, University of Padova.

Conferences

- V Congress of the National Bioengineering Group (GNB), Naples;
- 39th Annual International Conference of IEEE Engineering in Medicine and Biology Society, Jeju Island, South Korea.

Research periods in foreign Universities

Period of permanence	27/03/2017 – 27/07/2017
Host facility	Institut de Neurosciences des Systèmes (INS, UMR1106)
University	Aix-Marseille Université
Supervisor	Christian Bénar

Participation in national and international research projects

1	Title of the research	SW DISCOVERY (Small World Discovery)
	Funding institution	Regione Lazio
	Central manager	SeA (Società Sicurezza e Automazione)
	Local scientific officer	Prof. Laura Astolfi
2	Title of the research	Brain Computer Interface-driven rehabilitation after stroke: an add-on intervention for hand motor recovery
	Funding institution	Ministero della salute
	Central manager	Dott.ssa Donatella Mattia
	Local S. officer	Prof.ssa Laura Astolfi

3	Title of the research	FIRB: Brain-to-brain connectivity from simultaneous neuroelectric and autonomic multi-subjects recordings as a new tool to study human social interaction
	Funding institution	MIUR (Ministero dell'Istruzione dell'Università e della Ricerca)
	Central manager	Prof.ssa Laura Astolfi
4	Title of the research	Measuring the impact of lesions in EEG source imaging
	Funding institution	Sapienza University of Rome
	Central manager	Stefano Caschera
	Local scientific officer	Stefano Caschera
5	Title of the research	NeuroNet: Realistic Modeling of Anatomo-Functional Conditions in EEG-based Brain Functional Connectivity
	Funding institution	Sapienza University of Rome
	Central manager	Stefano Caschera, Alessandra Anzolin

Scientific publications

Title: EEG source estimation accuracy in presence of simulated cortical lesions - DOI: 10.1109/EMBC.2017.8036882
Autors: **Caschera S.**, Petti M., Mattia D., Astolfi L.
Conference: 39th Annual International Conference of IEEE Engineering in Medicine and Biology Society, Jeju Island, South Korea

Title: An EEG Index of Sensorimotor Interhemispheric Coupling after unilateral stroke: clinical and neurophysiological study - DOI: 10.1111/ejn.13797
Autors: Pichiorri F., Petti M., **Caschera S.**, Cincotti F., Astolfi L., Mattia D.
Journal: European Journal of Neuroscience

Title: Estimating Brain Connectivity when few Data Points are Available: Perspectives and Limitations - DOI: 10.1109/EMBC.2017.8037819
Autors: Antonacci Y.,Toppi J., Anzolin A., **Caschera S.**, Mattia D., Astolfi L.
Conference: 39th Annual International Conference of IEEE Engineering in Medicine and Biology Society, Jeju Island, South Korea

Title: Effect of inter-trials variability on the estimation of cortical connectivity by Partial Directed Coherence - DOI: 10.1109/EMBC.2015.7319219
Autors: M. Petti, **S. Caschera**, A. Anzolin, J. Toppi, F. Pichiorri, F. Babiloni, F. Cincotti, D. Mattia e L. Astolfi
Conference: 37a Conferenza annuale Internazionale della IEEE Engineering in Medicine and Biology Society (EMBS), Milano, Italia

Title: Effective Interhemispheric Connectivity and Corticospinal Tract Integrity interdependency after unilateral stroke
Autors: F. Pichiorri, M. Petti, **S. Caschera**, L. Astolfi, F. Cincotti e D. Mattia
Conference: 46o Congresso della Società Italiana di Neurologia (SIN), Genova, Italia

Title: Resting state effective connectivity in stroke patients. An EEG study
Autors: **S. Caschera**, L. Astolfi, M. Petti, F. Cincotti e D. Mattia
Conference: 9th IEEE-EMBS International Summer School on Biomedical Signal Processing, Pavia, Italia

Title: Effective interhemispheric connectivity and corticospinal tract integrity interdependency after unilateral stroke

Autors: **S. Caschera**, F. Pichiorri, M. Petti, F. Cincotti, L. Astolfi and D. Mattia
Conference: Quinto Congresso del Gruppo Nazionale di Bioingegneria, Napoli

Title: Measuring the Agreement between Brain Connectivity Networks - DOI: 10.1109/EMBC.2016.7590642
Autors: J. Toppi, N. Sciaraffa, Y. Antonacci, A. Anzolin, **S. Caschera**, M. Petti, D. Mattia, L. Astolfi
Conference: 38th Annual International Conference of the IEEE Engineering in Medicine and Biology Society